

RATES OF SARS-COV-2 TRANSMISSION
AND VACCINATION IMPACT THE FATE
OF VACCINE-RESISTANT STRAINS

2021

BANCO DE **ESPAÑA**
Eurosistema

Documentos de Trabajo
N.º 2129

Simón A. Rella, Yuliya A. Kulikova, Emmanouil T.
Dermitzakis and Fyodor A. Kondrashov

**RATES OF SARS-COV-2 TRANSMISSION AND VACCINATION IMPACT
THE FATE OF VACCINE-RESISTANT STRAINS**

RATES OF SARS-COV-2 TRANSMISSION AND VACCINATION IMPACT THE FATE OF VACCINE-RESISTANT STRAINS

Simón A. Rella ^(*)

INSTITUTE OF SCIENCE AND TECHNOLOGY AUSTRIA

Yuliya A. Kulikova ^(**)

BANCO DE ESPAÑA

Emmanouil T. Dermitzakis ^(***)

UNIVERSITY OF GENEVA MEDICAL SCHOOL

Fyodor A. Kondrashov ^(*)

INSTITUTE OF SCIENCE AND TECHNOLOGY AUSTRIA

(*) Institute of Science and Technology Austria, 1 Am Campus, Klosterneuburg, 3400, Austria. Corresponding author FAK fyodor.kondrashov@ist.ac.at.

(**) Banco de España, calle de Alcalá, 48, 28014 Madrid, Spain.

(***) Department of Genetic Medicine and Development, University of Geneva Medical School, Geneva, Switzerland. Corresponding author ETD Emmanouil.Dermitzakis@unige.ch.

Acknowledgements: We thank Alexey Kondrashov, Nick Machnik, Raimundo Julian Saona Urmeneta, Gasper Tkacik and Nick Barton for fruitful discussions. We also thank participants of EvoLunch seminar at IST Austria and the internal seminar at the Banco de España for useful comments. The opinions expressed in this document are exclusively of the authors and, therefore, do not necessarily coincide with those of the Banco de España or the Eurosystem. ETD is supported by the Swiss National Science and Louis Jeantet Foundation. The work of FAK was in part supported by the ERC Consolidator grant (771209-CharFL).

Contributors: ETD and FAK formulated the question. SAR and YAK formulated the model. SAR programmed and ran the model. All authors jointly analyzed the results and wrote the manuscript.

Code availability: <https://github.com/Simon-Re/mut-vacc>

The Working Paper Series seeks to disseminate original research in economics and finance. All papers have been anonymously refereed. By publishing these papers, the Banco de España aims to contribute to economic analysis and, in particular, to knowledge of the Spanish economy and its international environment.

The opinions and analyses in the Working Paper Series are the responsibility of the authors and, therefore, do not necessarily coincide with those of the Banco de España or the Eurosystem.

The Banco de España disseminates its main reports and most of its publications via the Internet at the following website: <http://www.bde.es>.

Reproduction for educational and non-commercial purposes is permitted provided that the source is acknowledged.

© BANCO DE ESPAÑA, Madrid, 2021

ISSN: 1579-8666 (on line)

Abstract

Vaccines are thought to be the best available solution for controlling the ongoing SARS-CoV-2 pandemic. However, the emergence of vaccine-resistant strains may come too rapidly for current vaccine developments to alleviate the health, economic and social consequences of the pandemic. To quantify and characterize the risk of such a scenario, we created a SIR-derived model with initial stochastic dynamics of the vaccine-resistant strain to study the probability of its emergence and establishment. Using parameters realistically resembling SARS-CoV-2 transmission, we model a wave-like pattern of the pandemic and consider the impact of the rate of vaccination and the strength of non-pharmaceutical intervention measures on the probability of emergence of a resistant strain. As expected, we found that a fast rate of vaccination decreases the probability of emergence of a resistant strain. Counterintuitively, when a relaxation of non-pharmaceutical interventions happened at a time when most individuals of the population have already been vaccinated the probability of emergence of a resistant strain was greatly increased. Consequently, we show that a period of transmission reduction close to the end of the vaccination campaign can substantially reduce the probability of resistant strain establishment. These results, therefore, suggest the convenience of maintaining non-pharmaceutical interventions and prevention protocols throughout the entire vaccination period.

Keywords: SARS-CoV-2 transmission, vaccination, vaccine-resistant strains, SIR model, stochastic dynamics.

JEL classification: C02, I18.

Resumen

Se considera que las vacunas son la mejor solución para controlar la actual pandemia por SARS-CoV-2. Sin embargo, la proliferación de cepas resistentes a las vacunas puede ser demasiado rápida para que su aplicación alivie la propagación de la pandemia, así como sus consecuencias económicas y sociales. Para cuantificar y caracterizar el riesgo de este escenario, utilizamos un modelo SIR con una dinámica estocástica para estudiar la probabilidad de aparición y transmisión de cepas resistentes a la vacuna. Usando parámetros que repliquen de manera realista la transmisión del SARS-CoV-2, modelizamos el patrón en forma de olas de la pandemia y consideramos el impacto que el ritmo de vacunación y la intensidad de las medidas de contención adoptadas tienen sobre la probabilidad de aparición de cepas resistentes a la vacuna. Como era de esperar, un ritmo rápido de vacunación disminuye la probabilidad de aparición de una cepa resistente a la vacuna. Sin embargo, aunque en principio pueda parecer contraintuitivo, cuando se produce una relajación de las restricciones en el momento en el que la mayoría de la población ya ha sido vacunada, la probabilidad de aparición de una cepa resistente a la vacuna aumenta considerablemente. En consecuencia, un período de contención estricta de la transmisión cerca del final de la campaña de vacunación puede reducir sustancialmente la probabilidad del establecimiento de cepas resistentes a la vacuna. Estos resultados, por tanto, sugieren la conveniencia de mantener las medidas y los protocolos de prevención durante toda la duración de la campaña de vacunación.

Palabras clave: transmisión del SARS-CoV-2, vacunación, cepas resistentes a vacunas, modelo SIR, dinámica estocástica.

Códigos JEL: C02, I18.

Introduction

Vaccines are among the most effective public health measures against infectious disease¹. Their track record brings hope that SARS-CoV-2 may soon be under control² as a consequence of a plethora of vaccine development efforts³⁻⁸. A potential cause of concern is the low rate of vaccine production and administration⁹ coupled with reports of new strains with higher transmission rates¹⁰⁻¹² and even with potential for some degree of vaccine resistance¹³⁻¹⁶. A number of models considered the dynamics of the spread of a vaccine-resistant strain in the population¹⁷⁻²⁰. However, to our knowledge, the interplay of the population vaccination rate with the stochastic dynamics of emergence of a resistant strain has been discussed²¹, but not formally modeled. Specifically, a concern is whether a combination of vaccination and transmission rates can create positive selection pressure on the emergence and establishment of resistant strains^{22,23}. To address this issue, we implemented a model to simulate the probability of emergence of a resistant strain as a function of vaccination rates and changes in the rate of virus transmission, resembling those caused by non-pharmaceutical interventions and behavioural changes. We then performed a number of simulations based on realistic parameters to study the likelihood and pattern of the emergence of a resistant strain. Finally, we considered possible countermeasures to reduce the probability of the establishment of the resistant strain in the population.

Results

We implemented a modification of a SIR model^{18,24} that included additional states to study the interplay of the rate of vaccination, rate of transmission and the likelihood of emergence of resistant strains (**figure 1a**). In addition to other states, individuals could be vaccinated (V), infected by the resistant strain (I_r), or simultaneously be vaccinated and infected with the resistant strain (I_r^V). The model was run to simulate a population of 10,000,000 individuals over three years with the vaccination starting after the first year. In the model, the susceptible individuals (S) are infected by the wildtype, or the original, strain at a rate of β and infected individuals recover at a rate of γ or die at a rate of δ . At each time step, a fraction θ of all non-infected individuals is vaccinated and with some fixed probability p , an infected individual becomes infected with a resistant strain. Conversely, any individual infected with the resistant strain can revert back to the wildtype strain population with the same probability, p . Immunity acquired after infection decayed at a rate of μ . Overall, our model included 8 character states and 6 transition parameters between them (**figure 1a, Table 1**).

The rate of transmission in the course of a pandemic is typically cyclical²⁵⁻²⁷ due to government interventions^{27,28}, behavioural changes²⁹⁻³¹, and environmental^{32,33} and other factors^{34,35}. Generally, the number of infected individuals is wave-like, guided by periods of high rate of transmission, followed by periods of a low rate of transmission^{25,26,36,37}. We thus varied β , the rate of virus transmission to reflect this cyclical behavior (**figure 1b,c**). A high rate of transmission ($\beta_h = 0.18$, equivalent to the effective reproduction number of $R_h = 2.52$) was alternated with a low rate ($\beta_l = 0.055$ or $R_l = 0.77$), which broadly reflected the observed rates of transmission in various countries affected by the SARS-CoV-19 pandemic with and without lockdown measures, respectively³⁷⁻³⁹. The low rate of transmission was triggered in the model when the number of individuals infected with any strain reached a high threshold $F_h = (I_{wt} + I_r + I_r^V)$. We considered two modes of transition from a low rate of transmission back to a high rate, when the number of infected individuals reached a low threshold F_l at a constant value of $F_l = (I_{wt} + I_r + I_r^V) = 1000$, which was used to generate the main figures, and at a relative value of $F_l = F_h/8$, which are available as supplementary materials. The explored values of F_h and F_l were selected such that the number of infection waves during the first year of the model roughly coincided with the number of waves of SARS-CoV-2 infection observed in most countries during the first year of the pandemic.

SIR-like models frequently consider only deterministic dynamics¹⁸. However, the emergence of a new strain is an inherently stochastic process under extensive influence of genetic drift^{40,41}. Therefore, we incorporated a stochastic stage into our model to allow for genetic drift in the early phases of population dynamics of the resistant strains. The growth rate of the number of individuals infected with the wildtype strain at time t was determined deterministically by $(\beta * S/N - \gamma - \delta)I_{wt}$. By contrast, when the frequency of the resistant strain in the population is low, the number of transmissions of the resistant strain was drawn from a Poisson distribution with a mean of $(\beta I_r (S + V)/N)dt$ ^[42]. However, when the frequency of the resistant strain is greater than 1000 individuals (0.01% of the population), making it highly unlikely to disappear by stochastic forces, the dynamics are treated deterministically in the same manner as the wildtype strain.

We define three stages of vaccine-resistant strain propagation, including emergence, the appearance of the first individual with the infected strain, establishment, the time point when the number of infected individuals reached 1000, and extinction, when the number of resistant strain infected individuals returned to zero. The impact of three parameters on the resistant strain propagation were explored: the probability of the emergence of the resistant strain (p), the speed of vaccination (θ) and the initiation of periods of lower rate of transmission (F_h). All other parameters were constants and their values were chosen to be broadly reflecting a realistic set of parameters that approximate the available data for the SARS-CoV-2 pandemic, $\mu = 1/180$, $\gamma = 0.99 * 1/14$ and $\delta = 0.01 * 1/14$ (see **Table 1**).

Higher probability of the initial emergence of a resistant strain emerging in a single individual, p , had a predictably⁴³ positive effect on the probability of the establishment of the resistant strain (**figures S1-S3**), but depended on the rate of vaccination (θ) and low transmission initiation (F_h) in a complex manner (**figure 2, figures S1-S3**). The dependency was periodic and the probability of establishment of the resistant strain was different by a factor of two even for some similar values of θ and F_h (**figure 2d,e**).

The behaviour of the emergence, establishment and extinction of the resistant strain in the population bears striking resemblance to the population genetics problem addressing the survival of a beneficial allele in a growing population^{44,45}. To understand the stochastic dynamics of the resistant strain in the model, it is therefore instructive to consider the underlying mechanism in population genetics terms. Unless the rate of mutation is zero, or infinitesimally low, new variants will emerge in the population at a rate of $p * I_{wt}$. When the rates of transmission of the wildtype and the resistant strain are equal, the probability that the resistant strain will go extinct, $1 - Q_t$, can be approximated by

$$1 - Q_t = \exp[-Q_{t+1}(1 + s)R_t^r] \text{ (eq.1),}$$

where s is the selection advantage of the resistant strain^{40,46} and $R_t^r = (S+V)\beta/N(\gamma + \delta)$, or the rate of population growth. Therefore, even when there is no selective advantage of the resistant strain ($s = 0$) over the wildtype strain but the rate of transmission is high ($R_t^r > 1$), the likelihood that a new mutation is lost from the population is small ($\sim 10\%$ for $\beta_h = 0.18$, or $R_0 = 2.52$). By contrast, when the rate of transmission is low ($R_t^r < 1$, which is the case during the low transmission periods in the model), the probability of extinction of the resistant strain by genetic drift is substantial^{40,41}. The results of our model are consistent with theory^{40,41}, such that the resistant strain emerges during periods of high and low transmission rates, but goes extinct with higher probability during periods of low transmission (**figure 2f**). Furthermore, under the parameters of our model the resistant strain becomes established only when the rate of transmission is high (**figure 2f**).

The complex influence of the speed of vaccination, θ , and initiation of low transmission period, F_h , on the dynamics of establishment of the resistant strain (**figure 2d**) is, therefore, likely driven by the overlap of the vaccination period and the periodicity of the cycles of the number of infected individuals driven by the interaction of F_h and θ (**figure 1b,c**). The coincidence of a high number of vaccinated individuals and a high rate of transmission has two effects on the resistant strain. First, as mentioned previously, because the rate of transmission is high, the emerging resistant strain is not lost through genetic drift (see also^{44,47}). Second, a high number of vaccinations creates a selective advantage of the resistant strain over the wildtype strain²³. The effective reproductive number of the wildtype versus the resistant strains, R_t^{wt}/R_t^r , is $(V+S)/S$, which is the selective advantage $1+s$ in **eq. 1**. Thus, when V is large the resistant strain has a growth advantage over the wildtype strain, contributing to its establishment in the population towards the end of the vaccination campaign. Taken together, the highest probability for establishment of the resistant strain for a given p is reached when V , I_{wt} and β (and the corresponding R_t^r) are large (**figure 2c, eq. 1**).

Indeed, when $p = 10^{-6}$, in those cases when the resistant strain becomes established, its initial time of emergence frequently occurs at around the time when 60% of the population is vaccinated (**figure 3**). Therefore, we then tested the influence of a single intervention triggering at a single extraordinary period of low transmission centred around 60% of vaccinated individuals in the population (**figure 3**). We varied the duration of this intervention, T , ranging from one week to 120 days and considered three rates of transmission, $\beta_t = 0.055$ ($R_0 = 0.77$), 0.03 ($R_0 = 0.42$) and 0.01 ($R_0 = 0.14$). Both parameters decrease the probability of establishment of the resistant strain with the length of the intervention having a relatively stronger effect (**figure 3, figures S1-S7**).

Discussion

Our model suggests three specific risk factors that favour the emergence and establishment of a vaccine-resistant strain that are intuitively obvious: high probability of initial emergence of the resistant strain, high number of infected individuals⁴⁸ and low rate of vaccination⁴⁹. By contrast, a counterintuitive result of our analysis is that the highest risk of resistant strain establishment occurs when a large fraction of the population has already been vaccinated but the transmission is not controlled. Similar conclusions have been reached in a SIR model of the ongoing pandemic⁵⁰ and a model of pathogen escape from host immunity⁵¹. Furthermore, empirical data consistent with this result has been reported for influenza⁵². Indeed, it seems likely that when a large fraction of the population is vaccinated, especially the high-risk fraction of the population (aged individuals and those with specific underlying conditions) there will be a drive to return to pre-pandemic guidelines⁵³ and behaviours conducive to a high rate of virus transmission^{54,55}. However, the establishment of a resistant strain at that time may lead to serial rounds of resistant strain evolution with vaccine development playing catch up in the evolutionary arms race against novel strains.

Prior to discussion of the implications of our model we reflect on several properties of the assumptions and implementation of our model. In classical SIR-like deterministic models even a single individual infected with a vaccine resistant strain with reproduction number $R_t > 1$ will lead to automatic establishment of the strain in the population. In an analytical solution, a SIR-like model, even for $R_t < 1$ for the vaccine resistant strain, the number of infected individuals will tend to 0 but only as time tends to infinity. In actual populations, a single individual infected with a vaccine resistant strain still has a non-negligible chance not to infect anyone causing the variant to go extinct due to random stochastic forces⁴¹. Therefore, the implementation of stochastic

dynamics^{56,57} of the vaccine resistant strain at low frequency in our model, considers the impact of random drift on its dynamics, which lies at the heart of extinction of rare strains.

We considered the dynamics of a single vaccine resistant strain, however, there may be different mutations that can lead to vaccine resistance. The emergence of different genotypes causing the same phenotype is analogous to a distinction in population genetics between alleles identical by state and by descent⁵⁸. In our model, the treatment of independent emergence of different mutations as a single entity does not influence the dynamics under the following two assumptions. First, that different mutations lead to exactly the same phenotype, which is vaccine resistance, and, second, that there is no recombination. However, the reported dynamics may be quantitatively different if either of the two assumptions do not hold.

We have not explored the parameter ranges of β_h , β_l , the high and low rates of transmission, respectively, and F_l the threshold between low and high rate of transmission. We selected the β_h and β_l , to represent the known transmission values at the start of the pandemic³⁷⁻³⁹. However, evolving strains are reported to have a higher rate of transmission⁵⁹ leading to higher β_h and, possibly, β_l values than we used. An increase in the rate of transmission is not expected to qualitatively influence the reported dynamics, but would shift the probability density of establishment of a resistant strain (**figure 3**). Indeed, the peak probability at 60% vaccinated individuals roughly corresponds to the point at which for the given β_h , R_t , the average number of transmissions for one infected individual, becomes less than 1. Because the reproduction number for the vaccine resistant strain, R_t , is equal to $(S+V)\beta/N(\gamma + \delta)$, the perk of the risk of establishment of the vaccine resistant strain would increase proportional to an increase of β . An increase in either F_h or F_l would lead to more individuals becoming infected and a proportionally higher rate of emergence of the vaccine related strain, but would not change the qualitative behaviour of the model. Furthermore, an increase of F_l would lead to reversion to a high transmission rate with higher number of infected individuals, leading to shorter periods of low transmission and decreased probability of extinction of the vaccine resistant strains.

The results of our model provide several qualitative implications for the strategy forward in the months of vaccination. In our model, the probability of emergence of a resistant strain in one individual per day was in the range of 10^{-5} to 10^{-8} for a population of 10^7 individuals. For the entire human population of $\sim 10^{10}$ that probability would be 10^{-8} to 10^{-11} , which does not seem improbably large. As of February 2021, $\sim 10^9$ individuals have been infected by SARS-CoV-2^[60] with an average 14 days of sickness per individual⁶¹, so $>10^{10}$ number of total days of infected individuals. Furthermore, highly mutated strains may emerge as a result of long shedding in immunocompromised individuals, a rare but realistic scenario⁶²⁻⁶⁴. Taken together, the emergence of a partially or fully vaccine-resistant strain and its eventual establishment appears inevitable. However, as vaccination needs to be ahead of the spread of such strains in similar ways to influenza²³, it is necessary to reduce the probability of establishment by a targeted effort to reduce the virus transmission rate towards the end of the vaccination period before the current vaccines become ineffective. Conversely, lack of non-pharmaceutical interventions at that time can increase the probability of establishment of vaccine-resistant strains. For example, plans to vaccinate individuals with a high risk of a fatal disease outcome followed by a drive to reach herd immunity while in uncontrolled transmission among the rest of the population is likely to greatly increase the probability that a resistant strain is established, annulling the initial vaccination effort. Another potential risk factor may be the reversion of vaccinated individuals to pre-pandemic behaviours that can drive the initial spread of the resistant strain.

One simple specific recommendation is to keep transmission low even when a large fraction of the population has been vaccinated by implementing acute non-pharmaceutical interventions (i.e. reinforced social distancing measures) for a reasonable period of time, to allow emergent lineages of resistant strains to go extinct through stochastic genetic drift. The implementation of non-pharmaceutical measures at a time of high vaccination can also help reduce infectivity when the efficacy of vaccines is not perfect⁶⁵. Additional factors that may make these measures even more effective are: (i) increased and widespread testing, (ii) rigorous contact tracing, (iii) high rate of viral sequencing of positive cases^{52,66} and (iv) travel restrictions. Finally, while our model formally considers only one homogenous population, our data also suggest that delays in vaccination in some countries relative to others will make the global emergence of a vaccine-resistant strain more likely. Without global coordination, vaccine resistant strains may be eliminated in some populations but could persist in others. Thus, a truly global vaccination effort may be necessary to reduce the chances of a global spread of a resistant strain.

Materials and Methods

Our extension of the SIR Model features 8 distinct states. Susceptible, S , and recovered, R , individuals are vaccinated over time to become vaccinated, V , or recovered vaccinated, R^V , respectively. Susceptible individuals can become infected with the wildtype, I_{wt} , or the resistant virus strain, I_r . While the vaccinated population is immune to the wildtype, it can be infected by the vaccine-resistant strain, in which case the state is represented by I_r^V . After a while any infected individual recovers or dies, D . Finally, we assume that the recovered population retains natural immunity towards both strains, but becomes susceptible again with some small rate, μ . In our model, immunity against the wildtype strain gained through vaccination is not lost during the entire model period of 3 years, consistent with current estimates^{67,68}.

The total number of individuals, N , in the population remains constant at 10,000,000, which includes the diseased individuals. We do not introduce new individuals into the population because only a very small number of individuals die during the 3 years that we simulate.

$$S + I_{wt} + I_r + I_r^V + R + R^V + D + V = N \quad (\text{eq. 2})$$

For all of the 8 states, for convenience we omit time index, e.g. we write, for example, S instead of $S(t)$. In the limit of large population sizes, the full dynamics without mutations can be described by the following set of differential equations. In these equations, $\dot{x} = dx/dt$ where t is time.

$$\dot{S} = \mu R - \theta(t)S - \beta(t)(I_{wt} + I_r + I_r^V)S \quad (\text{eq. 3})$$

$$\dot{I}_{wt} = -(\gamma + \delta)I_{wt} + \beta(t)SI_{wt} \quad (\text{eq. 4})$$

$$\dot{I}_r = -(\gamma + \delta)I_r + \beta(t)S(I_r + I_r^V) \quad (\text{eq. 5})$$

$$\dot{I}_r^V = -(\gamma + \delta)I_r^V + \beta(t)V(I_r + I_r^V) \quad (\text{eq. 6})$$

$$\dot{R} = -\mu R - \theta(t)R + \gamma(I_{wt} + I_r) \quad (\text{eq. 7})$$

$$\dot{R}^V = -\mu R^V + \theta(t)R + \gamma I_r^V \quad (\text{eq. 8})$$

$$\dot{D} = \delta(I_{wt} + I_r + I_r^V) \quad (\text{eq. 9})$$

$$\dot{V} = \mu R^V + \theta(t)S - \beta(t)I_r V \quad (\text{eq. 10})$$

Or, in the matrix format, $\dot{X} = \hat{P}X$, with $X = (S, I_{wt}, I_r, I_r^V, R, R^V, D, V)^T$

$$\hat{P} = \begin{bmatrix} -\theta(t) & -\beta(t)S & -\beta(t)S & -\beta(t)S & \mu & 0 & 0 & 0 \\ \beta(t)I_{wt} & -(\gamma + \delta) & 0 & 0 & 0 & 0 & 0 & 0 \\ \beta(t)I_r & 0 & -(\gamma + \delta) - \beta(t)S & 0 & 0 & 0 & 0 & 0 \\ 0 & 0 & \beta(t)V & -(\gamma + \delta) & 0 & 0 & 0 & \beta(t)I_r^V \\ 0 & \gamma & \gamma & 0 & -(\mu + \theta(t)) & 0 & 0 & 0 \\ 0 & 0 & 0 & \gamma & \theta(t) & -\mu & 0 & 0 \\ 0 & \delta & \delta & \delta & 0 & 0 & 0 & 0 \\ 0 & 0 & -\beta(t)V & 0 & 0 & \mu & 0 & 0 \\ \theta(t) & 0 & 0 & 0 & 0 & 0 & 0 & 0 \end{bmatrix} \quad (\text{eq. 11})$$

The dynamics are influenced by the following constant parameters: the recovery rate, γ , the death rate, δ , and the rate at which natural immunity is lost, μ . Additionally we introduce a time dependent transmission rate $\beta(t)$ and a function $\theta(t)$, which controls the speed of vaccination.

Time Dependent Transmission Rate

Pandemics often proceed in wave-like pattern^{25,26,36,37}, so we introduce a parameter $\beta(t)$, which switches between high and low transmission rates. The model begins with a period of a high rate of transmission, β_h/N . A low transmission rate, β_l/N , is initiated when the fraction of individuals infected with any strain, $I = (I_{wt} + I_r + I_r^V)$, reaches the value of F_h . Transition from a period of low to high infection rate occurs at $F_l = 1000$ or $F_l = F_h/8$.

Vaccination

Vaccination is modelled as almost always a linear function with saturation. The deviation from linearity occurs towards the end of the vaccination period. At that time, there may be fewer individuals that can be vaccinated than the number of individuals vaccinated at any time point, or $S + R - h < \theta$. This state can persist for longer than one point in time because in our model infected individuals are vaccinated only once they recover. h denotes the number of individuals in the population that are never vaccinated. A maximum of $N-h$ individuals can be vaccinated at the end of the vaccination program. The constant k controls the saturation of the vaccination speed once the number of susceptible individuals is significantly depleted. The state dependent vaccination speed $\theta(t)$ is given as:

$$\theta(t) = \left(1 - \frac{h}{S+R+I_{wt}+I_r}\right) \left(\frac{\theta_0}{S+R+k}\right), \quad (\text{eq. 12})$$

where θ_0 can take different values and h and k are chosen to be small (see **Table 1**).

Integration Method

The deterministic differential equations **eq. 11** were numerically solved using an Euler Forward Integration Scheme, with time step Δt , measured in days.

Resistant Strain

Each day and for every individual infected with the wildtype strain, I_{wt} , there is a small probability p , that a vaccine-resistant strain emerges in that individual. Then this individual switches from state I_{wt} to state I_r . Conversely, any individual infected with the resistant strain, I_r , can revert back to the wildtype strain, I_{wt} , with the same probability p . Each time step the number of individuals that transition between being infected with different strains is drawn from a Poisson distribution with mean $\Delta t p I_{wt}$, for transition to the resistant strain, or $\Delta t p I_r$, for reversion to the wildtype strain. The sum of Poisson distributed random variables is itself a Poisson distributed random variable with the mean corresponding to the sum of the means.

Stochastic and Deterministic Regimes

The population dynamics of a rare variant is an inherently stochastic process^{40,41}. We can formally treat the spread of a disease in our model as a stochastic birth-death process. In the following we illustrate this with the number of wildtype infections I_{wt} as an example. In each infinitesimally small time step dt , there is a probability $\beta S I_{wt} dt$, that the wildtype population I_{wt} grows by 1, $I_{wt} \rightarrow I_{wt} + 1$, while the susceptible population is decreased, $S \rightarrow S - 1$. Similarly, with probability $(\gamma + \delta) I_{wt} dt$, I_{wt} is reduced by 1, $I_{wt} \rightarrow I_{wt} - 1$, while the number of recovered or dead grows by 1. We carefully model small populations, $I_{wt} < N^*$, with N^* representing a small number of individuals, using a stochastic Tau-Leaping Algorithm⁶⁹. We choose a fixed time step size τ , that is equal to the time step of the Euler Integrator Δt . For very small I_{wt} Tau Leaping Algorithm can produce a negative population⁶⁹. This stems from the fact, that the number of events K that occur in time τ is drawn from a Poisson Distribution, that always assigns a non-zero probability for any $K > I_{wt}$. We reduce the chances of such a scenario, by solving the exact SSA Gillespie Algorithm when I_{wt} is below a critical size N^c ⁴².

For large I_{wt} , larger than some N^* , this stochastic process can be approximated with the limiting differential **eq. 4** and an Euler Integration Scheme. Once $I_{wt} \geq N^*$, we consider that the resistant strain of the virus is established in the population and we continue modelling it using the deterministic equation¹⁸.

Parallel Evaluation Of Deterministic And Stochastic Variables

In our model we evaluate deterministic and the stochastic dynamics in parallel. While small populations of infected individuals are treated as stochastic, other variables, such as the number of susceptible individuals, S , are evaluated within the deterministic regime. While the infection numbers of the wildtype or the emergent strain are in the stochastic regime ($< N^*$), the corresponding terms that contain the wildtype infections I_{wt} or the emergent infections I_r and I_r^V are removed from the deterministic rate equations. When I_{wt} or $I_r + I_r^V$ grow above the threshold value N^* , the corresponding population of infected individuals is treated as deterministic.

Sources of Errors

Finally, we discuss some sources of errors in our simulation: (1) Depending on the time step Δt the Euler Integration Scheme is not exact. In most of our simulations, we choose a time step of one day, $\Delta t = 1d$. (2) Using the deterministic rate equations for the infection numbers in **eq. 11** is an approximation to the exact stochastic dynamics given by a birth-death model. The quality of this approximation is given by the threshold value N^* , which was 1000 in our model. (3) When I_{wt}

or $I_r + I_r^V$ trespasses the threshold N^* from above, the populations of infected individuals changes from being treated as a real number (the mean field average) to being treated as a natural number. We truncate the mean field average with a floor function and treat the remainder as part of the recovered population. (4) The Tau Leaping algorithm is an approximation to the exact SSA Gillespie Algorithm, that allows faster evaluation with a constant step size τ . Increasing the threshold value N_c increases the accuracy of the model (**figure S12**). (5) As discussed above, on rare occasions a population of infected individuals drops below 0 in one leap. If this happens we redraw from the same Poisson distribution. (6) Finally, while the time step of the deterministic model Δt and τ are chosen to be equal, for population sizes above N_c , the SSA algorithm acts on exponentially distributed waiting times τ_{SSA} between reactions⁴². This introduces errors, if $\tau_{SSA} \gg \Delta t$, because the interaction rates may change, while we wait for the next reaction to occur.

In order to determine a range of acceptable values of N_c , we ran our simulation for a period of $T=200$ days, initially loading the system with $I_{wt} = 200$ wildtype carriers. For multiple values of N_c and no mutations, we compared the results of disease survival with the analytical solution derived for the birth death process,

$$P(I_{wt}(T) = 0) = 1 - \left(\frac{(\delta+\gamma)e^{(\delta+\gamma-\beta)T} - \gamma - \delta}{(\delta+\gamma)e^{(\delta+\gamma-\beta)T} - \beta} \right)^{I_{wt}(0)}. \quad (\text{eq. 13})$$

We pick $N_c=100$ individuals, which gives us a reasonably small error.

Assumptions and Choice of Parameters

The model is run for a total time of three years, with vaccination starting one year into the model. We assume that the wildtype and emergent strains have the same infectivity (β is the same for both strains). We assume that infection by any one strain provides immunity to both, reflecting that many vaccines carry only the Spike protein of the SARS-CoV-2 virus and it may be easier to escape immunity provided by the vaccine than the immunity provided by infection. We also assume that the immune response provided by the vaccine is more permanent and that immunity provided by infection, is lost at rate μ , *on average* after 0.5 years^{2,67,68,70} after recovery. Both of these assumptions influence the model when the number of infected individuals becomes large, which is unlikely for realistic average rates of transmission across the simulated time.

We assume that susceptible and recovered individuals have an equal chance to be vaccinated, θ_0 . We also assume that the infection-recovery rate, γ , and infection-fatality rate, δ are the same for the wildtype and mutated strains.

We regulate the rates of transmission exogenously in the model, with the rate of transmission (β) switching between a high rate, β_h and a low rate, β_l , when the total number of individuals infected with either strain reaches a threshold parameter. These threshold parameters, F_h and F_l , simultaneously reflect the impact of all non-pharmaceutical interventions and behavioural changes of individuals. The ranges of these parameters were chosen to broadly reflect realistic parameters of a pandemic, including rates of infection and several waves of high infection in the first couple of years of the model.

We operate under the assumption that vaccine efficacy not only impacts disease manifestation but also blocks transmission at the same rate, which is a reasonable assumption based on previous vaccine performance but has not yet been demonstrated.

In **Table 1** we present the choice of parameters for the model, the ones that were constant and those that were varied, including their boundaries.

References

Adak, D., A. Majumder and N. Bairagi (2021). "Mathematical perspective of Covid-19 pandemic: Disease extinction criteria in deterministic and stochastic models", *Chaos Solitons Fractals*, No. 142, p. 110381.

Aleta, A., *et al.* (2020). "Modeling the impact of social distancing, testing, contact tracing and household quarantine on second-wave scenarios of the COVID-19 epidemic", *medRxiv*, doi: 10.1101/2020.05.06.20092841.

Alimohamadi, Y., M. Taghdir and M. Sepandi (2020). "Estimate of the Basic Reproduction Number for COVID-19: A Systematic Review and Meta-analysis", *J. Prev. Med. Public Health*, No. 53, pp. 151-157.

Anderson, R. M., C. Vegvari, J. Truscott and B. S. Collyer (2020). "Challenges in creating herd immunity to SARS-CoV-2 infection by mass vaccination", *Lancet*, No. 396, pp. 1614-1616.

Andre, F. E., *et al.* (2008). "Vaccination greatly reduces disease, disability, death and inequity worldwide", *Bull. World Health Organ.*, No. 86, pp. 140-146.

Andreano, E., *et al.* (2020). "SARS-CoV-2 escape in vitro from a highly neutralizing COVID-19 convalescent plasma", *bioRxiv*, doi: 10.1101/2020.12.28.424451.

Avanzato, V. A., *et al.* (2020). "Case Study: Prolonged Infectious SARS-CoV-2 Shedding from an Asymptomatic Immunocompromised Individual with Cancer", *Cell*, Vol. 183, pp. 1901-1912.e9.

Baden, L. R., *et al.* (2021). "Efficacy and Safety of the mRNA-1273 SARS-CoV-2 Vaccine", *N. Engl. J. Med.*, No. 384, pp. 403-416.

Barnes, C. O., *et al.* (2020). "SARS-CoV-2 neutralizing antibody structures inform therapeutic strategies", *Nature*, No. 588, pp. 682-687.

Bavel, J. J. van, *et al.* (2020). "Using social and behavioural science to support COVID-19 pandemic response", *Nat Hum Behav*, No. 4, pp. 460-471.

Bazykin G. A., O. Stanevich, D. Danilenko, A. Fadeev, K. Komissarova, A. Ivanova, M. Sergeeva, K. Safina, E. Nabieva, G. Klink, S. Garushyants, J. Zabutova, A. Kholodnaia, I. Skorokhod, V. V. Ryabchikova, A. Komissarov, D. Lioznov (2021).

“Emergence of Y453F and Δ 69-70HV mutations in a lymphoma patient with long-term COVID-19”, https://virological.org/t/emergence-of-y453f-and-69-70hv-mutations-in-a-lymphoma-patient-with-long-term-covid-19/580?fbclid=IwAR0fMWUrXHqEhpU0j0LI_-cWuF4G-PbC_qAZWtqkZce943OffhdkLyNoFzw.

Bjørnstad, O. N., K. Shea, M. Krzywinski and N. Altman(2020). “Modeling infectious epidemics”, *Nat. Methods*, No. 17, pp. 455-456.

Bjørnstad, O. N., and C. Viboud (2016). “Timing and periodicity of influenza epidemics”, *Proceedings of the National Academy of Sciences of the United States of America*, Vol. 113, pp. 12899-12901.

Boni, M. F. (2008). “Vaccination and antigenic drift in influenza”, *Vaccine*, 26 Suppl 3, C8-14.

Boni, M. F., J. R. Gog, V. Andreasen and F. B Christiansen (2004). “Influenza drift and epidemic size: the race between generating and escaping immunity”, *Theor. Popul. Biol.*, No. 65, pp. 179-191.

Cacciapaglia, G., C. Cot and F. Sannino (2020). “Second wave COVID-19 pandemics in Europe: a temporal playbook”, *Sci. Rep.*, No. 10, p. 15514.

Cao, Y., D. T. Gillespie and L. R. Petzold (2005). “Avoiding negative populations in explicit Poisson tau-leaping”, *The Journal of Chemical Physics*, Vol. 123, 054104.

Carleton, T., J. Cornetet, P. Huybers, K. C. Meng and J. Proctor (2021). “Global evidence for ultraviolet radiation decreasing COVID-19 growth rates”, *Proc. Natl. Acad. Sci. U. S. A.*, No. 118.

Cele, S., *et al.* (2021). “Escape of SARS-CoV-2 501Y. V2 variants from neutralization by convalescent plasma”, *medRxiv*.

Chabas, H., *et al.* (2018). “Evolutionary emergence of infectious diseases in heterogeneous host populations”, *PLoS Biol.*, No. 16, e2006738.

Charlesworth, B., and D. Charlesworth (2010). *Elements of Evolutionary Genetics*, Roberts & Company.

Choi, B., *et al.* (2020). “Persistence and Evolution of SARS-CoV-2 in an Immunocompromised Host”, *N. Engl. J. Med.*, No. 383, pp. 2291-2293.

Chowdhury, R., *et al.* (2020). “Dynamic interventions to control COVID-19 pandemic: a multivariate prediction modelling study comparing 16 worldwide countries” *Eur. J. Epidemiol.*, No. 35, pp. 389-399.

Coronavirus (COVID-19) Vaccinations. <https://ourworldindata.org/covid-vaccinations>.

COVID-19 map - Johns Hopkins Coronavirus Resource Center,
<https://coronavirus.jhu.edu/map.html>.

Davies, N. G., *et al.* (2020). “Estimated transmissibility and severity of novel SARS-CoV-2 Variant of Concern 202012/01 in England”, *medRxiv*.

Davies, N. G., *et al.* (2021). “Estimated transmissibility and impact of SARS-CoV-2 lineage B.1.1.7 in England”, *Science*, No. 372.

Dickens, B. L., *et al.* (2020). “Modelling lockdown and exit strategies for COVID-19 in Singapore”, *The Lancet Regional Health – Western Pacific*, No. 1.

Dong, Y., *et al.* (2020). “A systematic review of SARS-CoV-2 vaccine candidates”, *Signal Transduct Target Ther*, No. 5, p. 237.

Eichenbaum, M. S., S. Rebelo and M. Trabandt (2020). *The Macroeconomics of Epidemics*, <https://www.nber.org/papers/w26882>, doi:10.3386/w26882.

Elena, S. F. and R. Sanjuán (2005). “Adaptive value of high mutation rates of RNA viruses: separating causes from consequences” *J. Virol.*, No. 79, pp. 11555-11558.

Eshel, I. (1984). “On the survival probability of a slightly advantageous mutant gene in a multitype population: A multidimensional branching process model”, *Journal Of Mathematical Biology*, Vol. 19, pp. 201-209.

Faria, N. R. (2021). “Genomic characterisation of an emergent SARS-CoV-2 lineage in Manaus: preliminary findings”, <https://virological.org/t/genomic-characterisation-of-an-emergent-sars-cov-2-lineage-in-manauas-preliminary-findings/586>.

Fudolig, M., and R. Howard (2020). “The local stability of a modified multi-strain SIR model for emerging viral strains” *PLoS One*, No. 15, e0243408.

Flaxman, S., *et al.* (2020). “Estimating the effects of non-pharmaceutical interventions on COVID-19 in Europe”, *Nature*, No. 584, pp. 257-261.

- Gillespie, D. T. (2001). "Approximate accelerated stochastic simulation of chemically reacting systems", *The Journal of Chemical Physics*, Vol. 115, pp. 1716-1733.
- Gillespie, J. H. (2004). *Population Genetics: A Concise Guide*, JHU Press.
- Graham, B. S. (2020). "Rapid COVID-19 vaccine development", *Science*, No. 368, pp. 945-94.
- Grenfell, B. T., *et al.* (2004). "Unifying the Epidemiological and Evolutionary Dynamics of Pathogens", *Science*, No. 303, pp. 327-332.
- Habersaat, K. B., *et al.* (2020). "Ten considerations for effectively managing the COVID-19 transition", *Nat Hum Behav*, No. 4, pp. 677-687.
- Hartley, G. E., *et al.* (2020). "Rapid generation of durable B cell memory to SARS-CoV-2 spike and nucleocapsid proteins in COVID-19 and convalescence", *Sci Immunol.*, No. 5.
- Huppert, A., and G. Katriel (2013). "Mathematical modelling and prediction in infectious disease epidemiology", *Clinical Microbiology and Infection*, Vol. 19, pp. 999-1005.
- Haldane, J. B. S. (1927). "A Mathematical Theory of Natural and Artificial Selection", Part V: "Selection and Mutation", *Math. Proc. Cambridge Philos. Soc.*, No. 23, pp. 838-844.
- Hilton, J., and M. J. Keeling (2020). "Estimation of country-level basic reproductive ratios for novel Coronavirus (SARS-CoV-2/COVID-19) using synthetic contact matrices", *PLoS Comput. Biol.*, No. 16, e1008031.
- Khatri, B. S. (2020). "Stochastic extinction of epidemics: how long would it take for Sars-Cov-2 to die out without herd immunity?", *medRxiv*.
- Kissler, S. M., C. Tedijanto, E. Goldstein, Y. H. Grad and M. Lipsitch (2020). "Projecting the transmission dynamics of SARS-CoV-2 through the postpandemic period", *Science*, No. 368, pp. 860-868.
- Kiyuka, P. K., *et al.* (2018). "Human Coronavirus NL63 Molecular Epidemiology and Evolutionary Patterns in Rural Coastal Kenya", *J. Infect. Dis.*, No. 217, pp. 1728-1739.
- Lauer, S. A., *et al.* (2020). "The Incubation Period of Coronavirus Disease 2019 (COVID-19) From Publicly Reported Confirmed Cases: Estimation and Application", *Ann. Intern. Med.*, No. 172, pp. 577-582.

Liu, W., *et al.* (2006). "Two-year prospective study of the humoral immune response of patients with severe acute respiratory syndrome", *J. Infect. Dis.*, No. 193, pp. 792-795.

Logunov, D. Y., *et al.* (2021). "Safety and efficacy of an rAd26 and rAd5 vector-based heterologous prime-boost COVID-19 vaccine: an interim analysis of a randomised controlled phase 3 trial in Russia", *The Lancet*, doi:10.1016/s0140-6736(21)00234-8.

Luong, T. H. (2019). *Mathematical Modeling of Vaccinations: Modified SIR Model, Vaccination Effects, and Herd Immunity*, Portland State University, doi:10.15760/honors.712.

Makhoul, M., *et al.* (2020). "Epidemiological Impact of SARS-CoV-2 Vaccination: Mathematical Modeling Analyses", *Vaccines (Basel)*, No. 8.

Malone, B., *et al.* (2020). "Artificial intelligence predicts the immunogenic landscape of SARS-CoV-2 leading to universal blueprints for vaccine designs", *Sci. Rep*, No. 10, p. 22375.

Martínez, M. E. (2018). "The calendar of epidemics: Seasonal cycles of infectious diseases", *PLoS Pathog.*, No. 14, e1007327.

Mecenas, P., R. T. da R. M. Bastos, A. C. R. Vallinoto and D. Normando (2020). "Effects of temperature and humidity on the spread of COVID-19: A systematic review", *PLoS One* No. 15, e0238339.

Orr, H. A., and R. L. Unckless (2008). Population Extinction and the Genetics of Adaptation. *The American Naturalist*, Vol. 172, pp. 160-169.

Otto, S. P., and M. C. Whitlock (1997). "The probability of fixation in populations of changing size", *Genetics*, No. 146, pp. 723-733.

Pastor-Barriuso, R., *et al.* (2020). "Infection fatality risk for SARS-CoV-2 in community dwelling population of Spain: nationwide seroepidemiological study", *BMJ*, No. 371, m4509.

Petrova, V. N., and C. A. Russell (2018). "The evolution of seasonal influenza viruses", *Nature Reviews Microbiology*, Vol. 16, pp. 47-60.

Petersen, E., *et al.* (2020). "Comparing SARS-CoV-2 with SARS-CoV and influenza pandemics", *Lancet Infect. Dis.*, No. 20, pp. e238-e244.

Polack, F. P., *et al.* (2020). "Safety and Efficacy of the BNT162b2 mRNA Covid-19 Vaccine", *N. Engl. J. Med.*, No. 383, pp. 2603-2615.

Rauff, D., C. Strydom and C. Abolnik (2016). "Evolutionary consequences of a decade of vaccination against subtype H6N2 influenza", *Virology*, No. 498, pp. 226-239.

Rosenstrom, E., *et al.* (2021). "High-Quality Masks Reduce COVID-19 Infections and Deaths in the US", *medRxiv*, doi:10.1101/2020.09.27.20199737.

Rochman, N., Y. Wolf and E. Koonin (2021). "Substantial impact of post-vaccination contacts on cumulative infections during viral epidemics", *F1000Res.*, No. 10, p. 315.

Tang, F., *et al.* (2011). "Lack of peripheral memory B cell responses in recovered patients with severe acute respiratory syndrome: a six-year follow-up study", *J. Immunol.*, No. 186, pp. 7264-7268 .

Tegally, H., *et al.* (2021). "Sixteen novel lineages of SARS-CoV-2 in South Africa", *Nat. Med.*, doi:10.1038/s41591-021-01255-3.

Uecker, H. and J. Hermisson (2011). "On the Fixation Process of a Beneficial Mutation in a Variable Environment", *Genetics*, Vol. 188, pp. 915-930.

Volz, E. M., and X. Didelot (2018). "Modeling the Growth and Decline of Pathogen Effective Population Size Provides Insight into Epidemic Dynamics and Drivers of Antimicrobial Resistance", *Systematic Biology*, Vol. 67, pp. 719-728.

Wen, F. T., A. Malani and S. Cobey. "The beneficial effects of vaccination on the evolution of seasonal influenza", doi:10.1101/162545.

West, R., S. Michie, G. J. Rubin and R. Amlôt (2020). "Applying principles of behaviour change to reduce SARS-CoV-2 transmission", *Nat Hum Behav*, No. 4, pp. 451-459

Williams, T. C., and W. A. Burgers (2021). "SARS-CoV-2 evolution and vaccines: cause for concern?", *Lancet Respir Med*, doi:10.1016/S2213-2600(21)00075-8.

Xiao, Y., and S. M. Moghadas (2013). "Impact of viral drift on vaccination dynamics and patterns of seasonal influenza", *BMC Infect. Dis.*, No.13, p. 589.

Yang, W., *et al.* (2021). Estimating the infection-fatality risk of SARS-CoV-2 in New York City during the spring 2020 pandemic wave: a model-based analysis", *Lancet Infect. Dis.*, No. 21, pp. 203-212.

Table 1. Model parameters

Parameter	Value	Comments
Fixed parameters		
Population size, N	10,000,000 individuals	
Cut-off for stochastic mode, N^*	1,000	
Cut-off for Gillespie algorithm, N_c	100	
Recovery rate, γ	$0.99 \cdot 1/14$	Average disease duration is 14 days ⁶¹
Death rate, δ	$0.01 \cdot 1/14$	Infection-fatality rate is 1% ⁷¹⁻⁷³
Loss of immunity rate, μ	$1/180$	On average in 180 days ^{74,75}
Share of non-vaccinated, h	0.01	1% of population
Saturation parameter, k	0.01	
Transmission rate, $\beta = \{\beta_l, \beta_h\}$	{0.055, 0.18}	$R_0 = \{0.77, 2.52\}$ ³⁷⁻³⁹
Δt	1 day	
Varying parameters		
Bound for initiation of low transmission, F_h	2,000 to 20,000 individuals	
Bound for initiation of high transmission, F_l	1,000 or $F_h/8$ individuals	
Probability of emergence of resistant strain, ρ	$1e-8$ to $1e-5$	Daily for every infected
Vaccination speed, θ_o	0.001 to 0.015	0.1% to 1.5% daily

Figures and Figure Legends

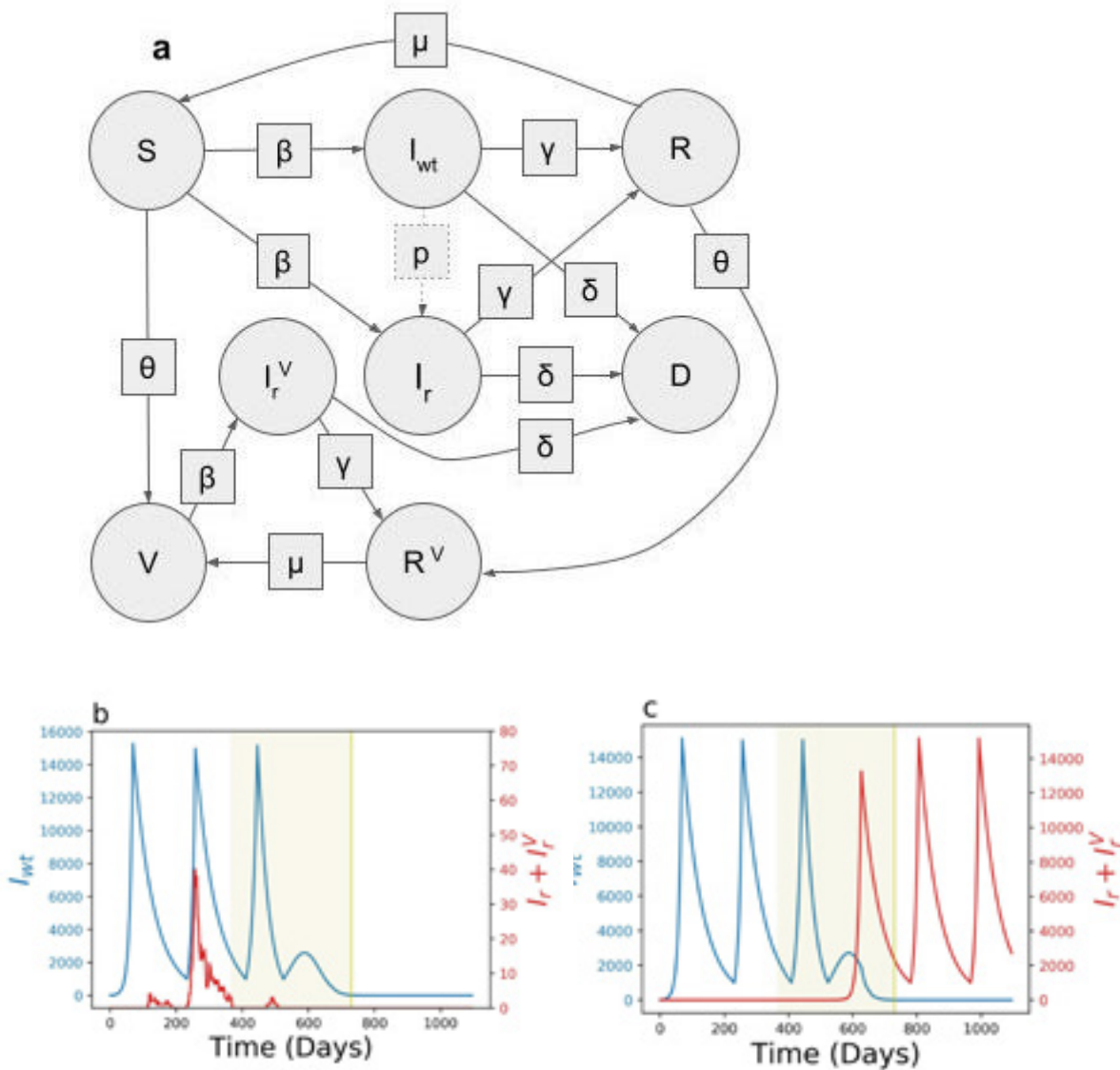


Figure 1. The states, transition parameters and dynamics. **a**, States are shown in circles and transition parameters in squares. The transition parameter, μ , is the rate at which individuals lose natural immunity and p , is the probability that an individual infected with the wildtype strain transmits a resistant strain, so it is not a deterministic parameter. Example dynamics of the number of individuals infected with the wildtype (blue) and resistant strains (red) for $p = 10^{-6}$, $\theta_0 = 1/365$ and $F_h = 15000$. The period of vaccination is highlighted (green). Under the same parameters the resistant strain may emerge and go extinct, **b**, or become established, **c**.

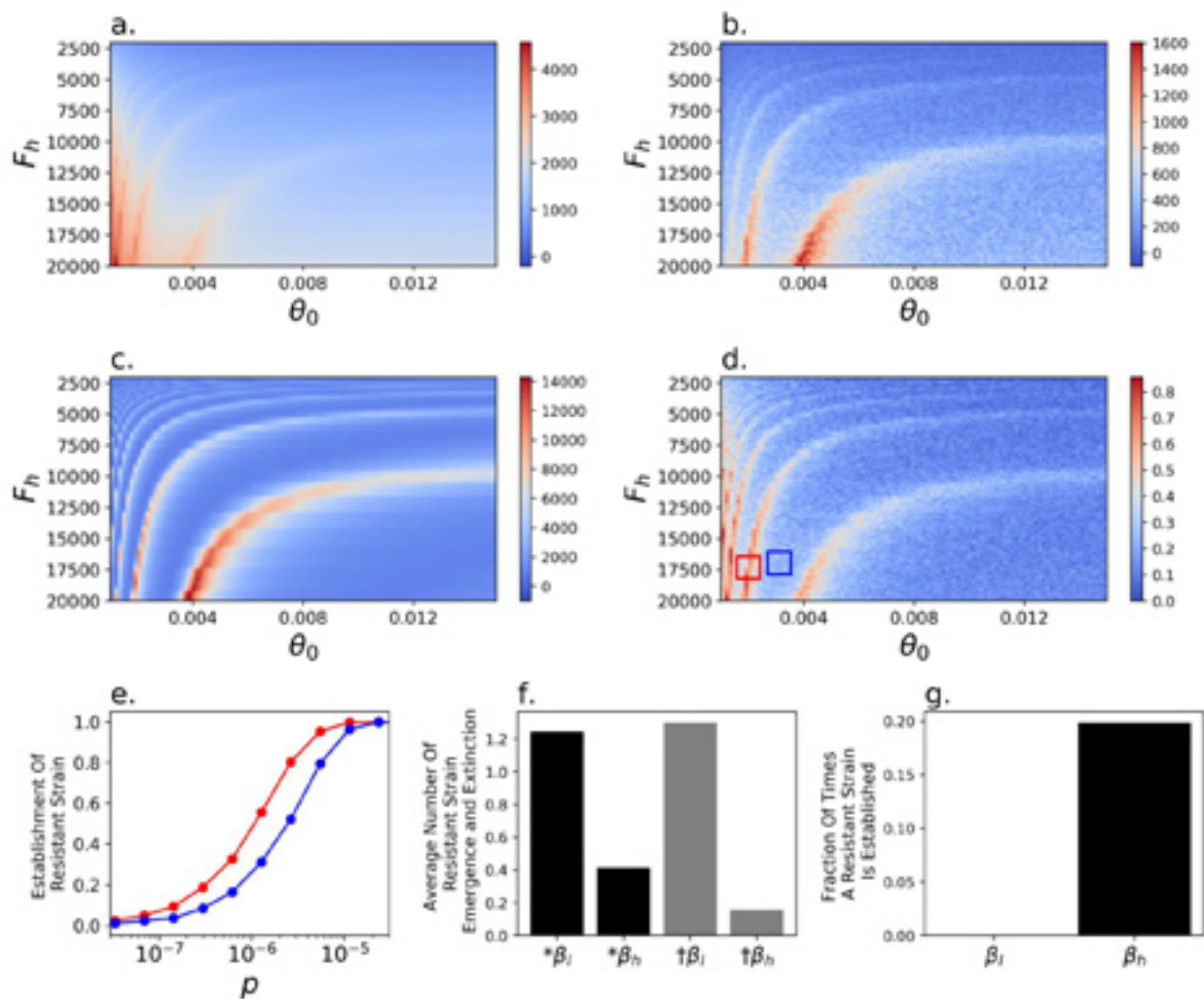


Figure 2. Impact of the rate of vaccination, θ , and the initiation of low rate of transmission, F_h , on model dynamics. The cumulative death rate from the **a**, wildtype and **b**, resistant strains, **c**, the number of wildtype-strain infected individuals at t_{v60} , the point in time when 60% of the population is vaccinated and **d**, the probability of resistant strain establishment, for $p=10^{-6}$. **e**, The probability of emergence of the resistant strain as a function of the probability of emergence, p shown for the parameter ranges of θ and F_h in the corresponding red and blue boxes from figure panel **d**. **f**, The average number of times of 8×10^6 simulation runs during which a resistant strain emerges (black) or goes extinct (grey) during periods of low (β_l) or high (β_h) transmission for $p = 10^{-6}$. **g**, A resistant strain was never observed to establish during periods of low transmission (β_l) for $p = 10^{-6}$.

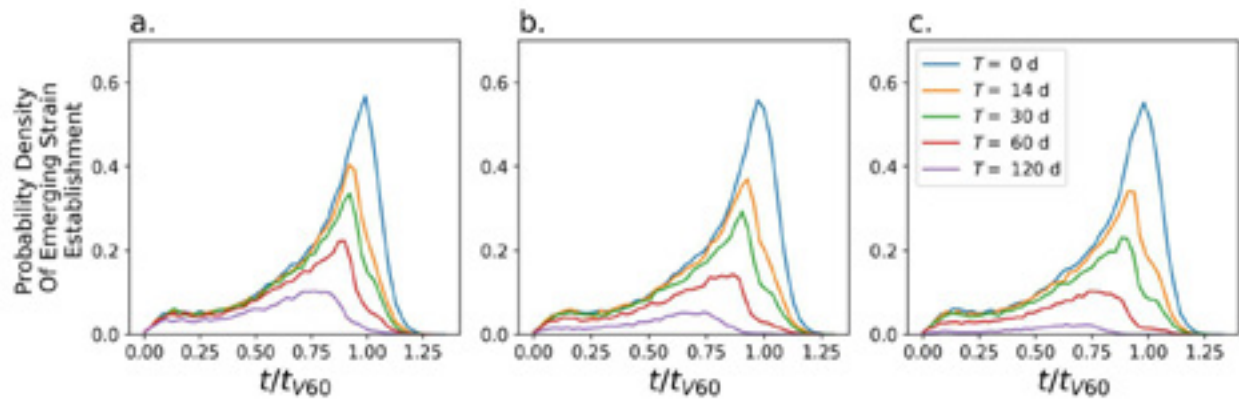


Figure 3. Time of initial emergence of a resistant strain that has become established. Probability density that the resistant strain emerges as a function of time since the start of the simulation, t , rescaled by the time at which 60% of the individuals are vaccinated, t_{v60} , averaged across simulations with θ (0.001 through 0.015), F_h (2,000 through 20,000) and $p = 10^{-6}$. Without any extraordinary periods of low transmission (blue line) the peak of the likelihood of emergence of a new strain is at $t/t_{v60} = 1$. The likelihood of emergence of a resistant strain can be reduced by an extraordinary period of low transmission centered at $t/t_{v60} = 1$ with a stronger reduction when such period is longer, T (colour-coded), or when the rate of transmission is more strongly reduced **a**, $\beta_i = 0.055$, **b**, $\beta_i = 0.03$, **c**, $\beta_i = 0.01$.

Supplementary Figures and Legends

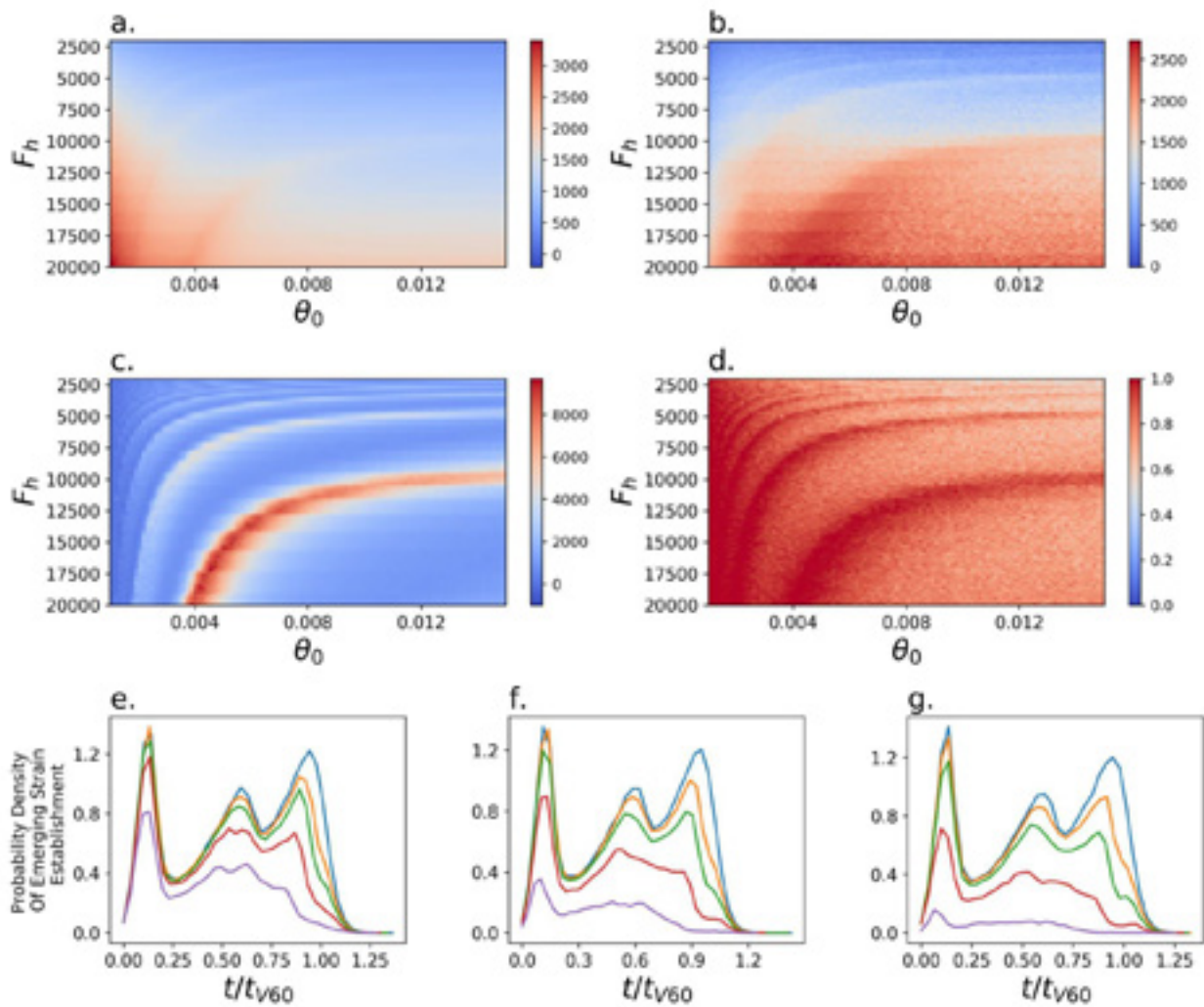


Figure S1 Impact of the rate of vaccination and initiation of low rate of transmission on model dynamics for $p = 10^{-5}$. The cumulative death rate from the **a**, wildtype and **b**, resistant strains, **c**, the number of wildtype-strain infected individuals at t_{v60} , the point in time when 60% of the population is vaccinated and **d**, the probability of resistant strain establishment. **e-g**, Probability density that the resistant strain emerges as a function of time since the start of the simulation, t , rescaled by the time at which 60% of the individuals are vaccinated, t_{v60} , summed across simulations with θ (0.001 through 0.015), F_h (2,000 through 20,000). The impact of the extraordinary low transmission period centered at $t/t_{v60} = 1$ on the likelihood of emergence of the resistant strain as a function of the duration of that period, T (colour-coded), and the intensity of the reduction of transmission **e**, $\beta_l = 0.055$, **f**, $\beta_l = 0.03$, **g**, $\beta_l = 0.01$.

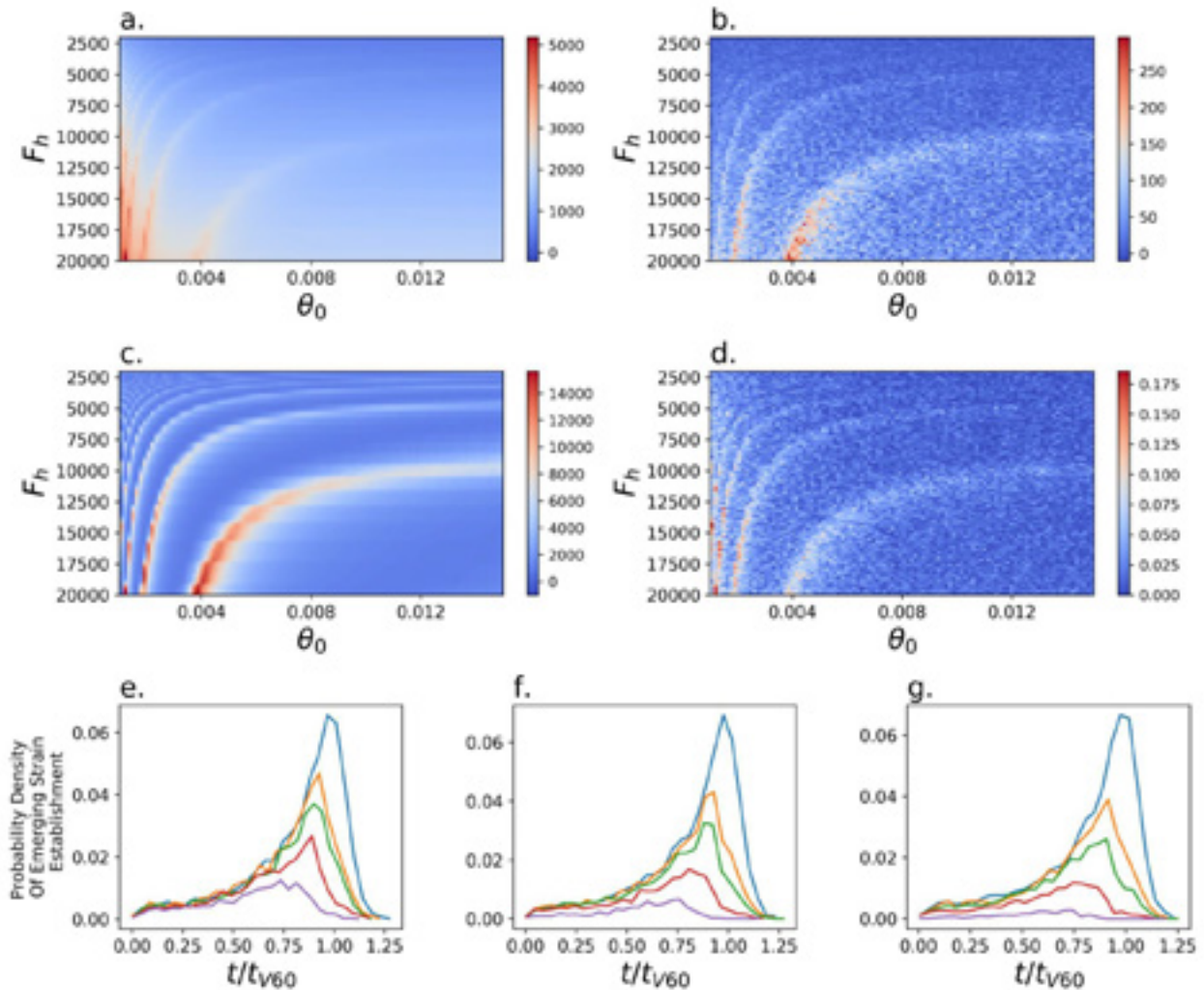


Figure S2 Impact of the rate of vaccination and initiation of low rate of transmission on model dynamics for $p = 10^{-7}$. The cumulative death rate from the **a**, wildtype and **b**, resistant strains, **c**, the number of wildtype-strain infected individuals at t_{v60} , the point in time when 60% of the population is vaccinated and **d**, the probability of resistant strain establishment. **e-g**, Probability density that the resistant strain emerges as a function of time since the start of the simulation, t , rescaled by the time at which 60% of the individuals are vaccinated, t_{v60} , summed across simulations with θ (0.001 through 0.015), F_h (2,000 through 20,000). The impact of the extraordinary low transmission period centered at $t/t_{v60} = 1$ on the likelihood of emergence of the resistant strain as a function of the duration of that period, T (colour-coded), and the intensity of the reduction of transmission **e**, $\beta_l = 0.055$, **f**, $\beta_l = 0.03$, **g**, $\beta_l = 0.01$.

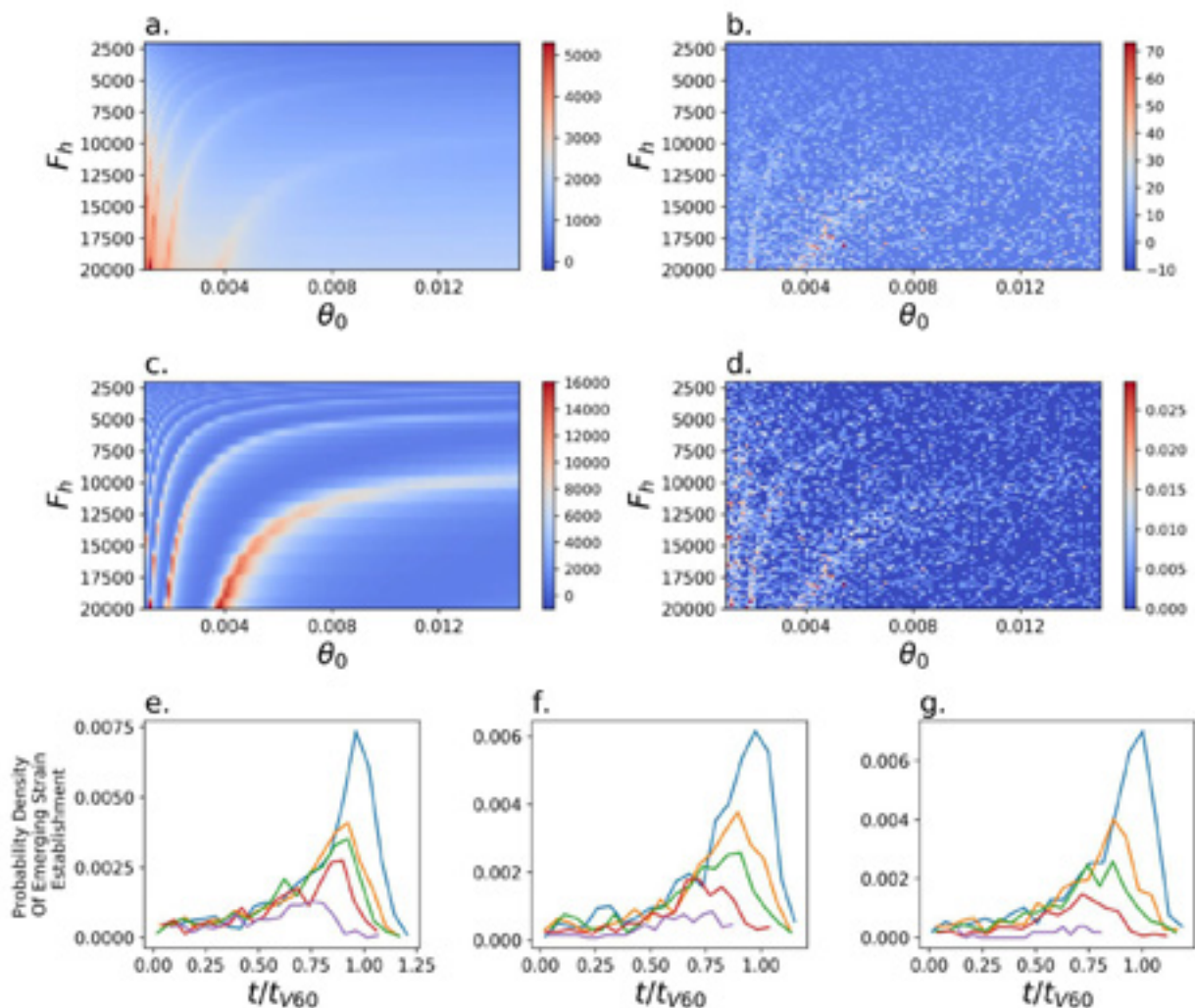


Figure S3 Impact of the rate of vaccination and initiation of low rate of transmission on model dynamics for $p = 10^{-8}$. The cumulative death rate from the **a**, wildtype and **b**, resistant strains, **c**, the number of wildtype-strain infected individuals at t_{v60} , the point in time when 60% of the population is vaccinated and **d**, the probability of resistant strain establishment. **e-g**, Probability density that the resistant strain emerges as a function of time since the start of the simulation, t , rescaled by the time at which 60% of the individuals are vaccinated, t_{v60} , summed across simulations with θ (0.001 through 0.015), F_h (2,000 through 20,000). The impact of the extraordinary low transmission period centered at $t/t_{v60} = 1$ on the likelihood of emergence of the resistant strain as a function of the duration of that period, T (colour-coded), and the intensity of the reduction of transmission **e**, $\beta_l = 0.055$, **f**, $\beta_l = 0.03$, **g**, $\beta_l = 0.01$.

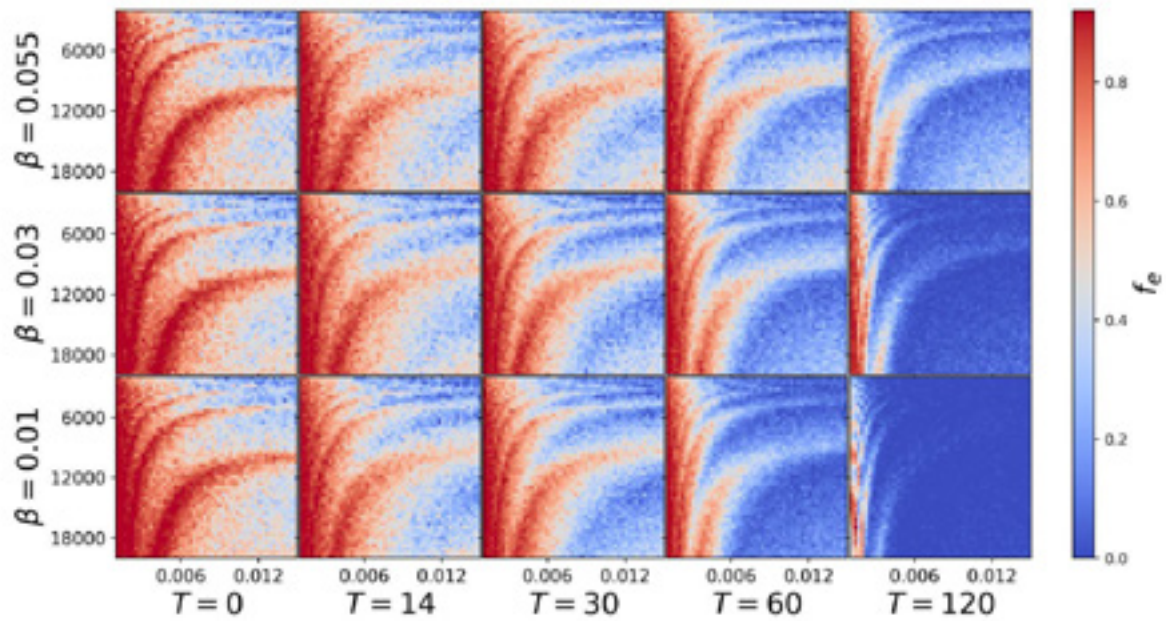


Figure S4 The probability of establishment of the resistant strain for $p = 10^{-5}$. The influence of low transmission period centered at $t/t_{v60} = 1$ on probability of establishment of the resistant strain as a function of the duration of that period, T , and the intensity of the reduction of transmission, β .

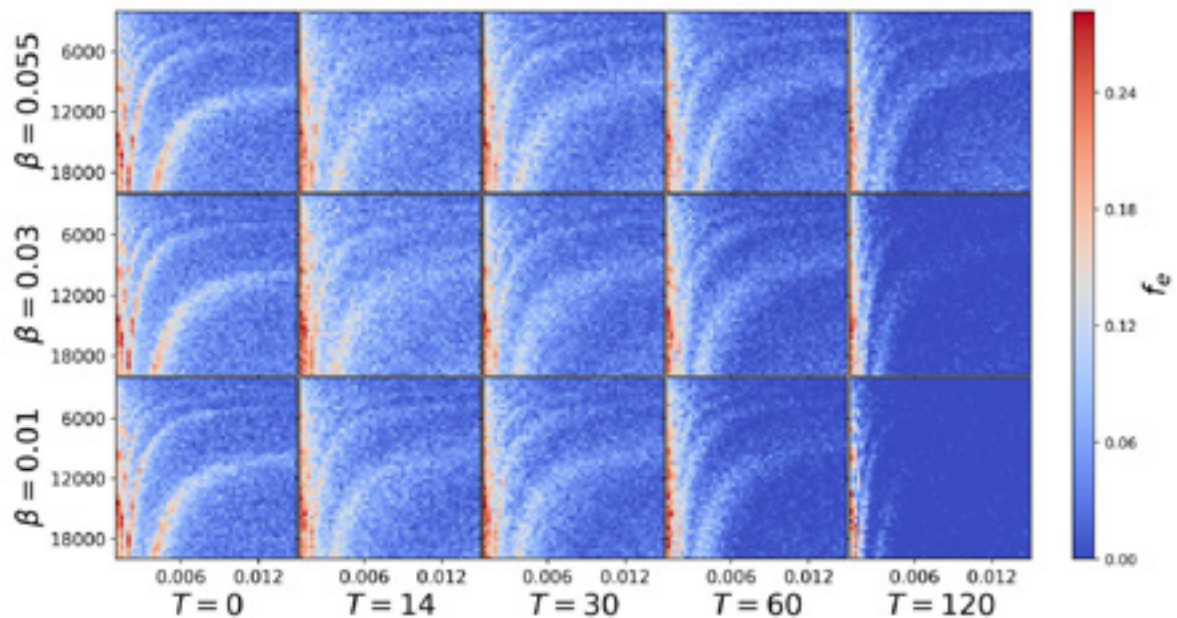


Figure S5 The probability of establishment of the resistant strain for $p = 10^{-6}$. The influence of low transmission period centered at $t/t_{v60} = 1$ on probability of establishment of the resistant strain as a function of the duration of that period, T , and the intensity of the reduction of transmission, β .

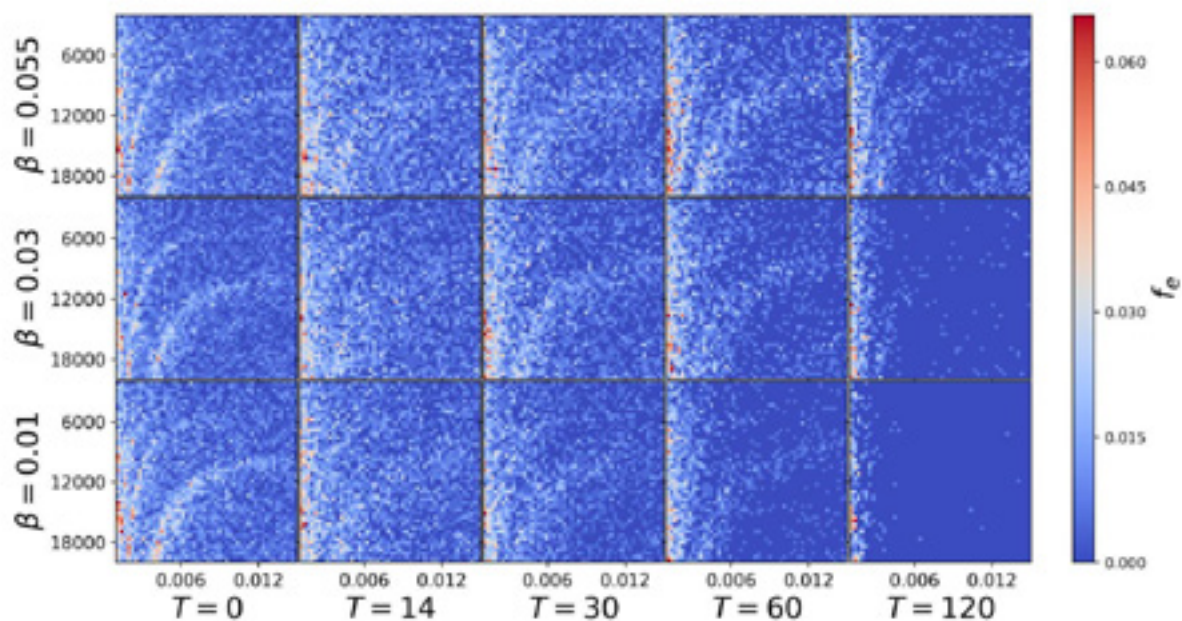


Figure S6 The probability of establishment of the resistant strain for $p = 10^{-7}$. The influence of low transmission period centered at $t/t_{v60} = 1$ on probability of establishment of the resistant strain as a function of the duration of that period, T , and the intensity of the reduction of transmission, β .

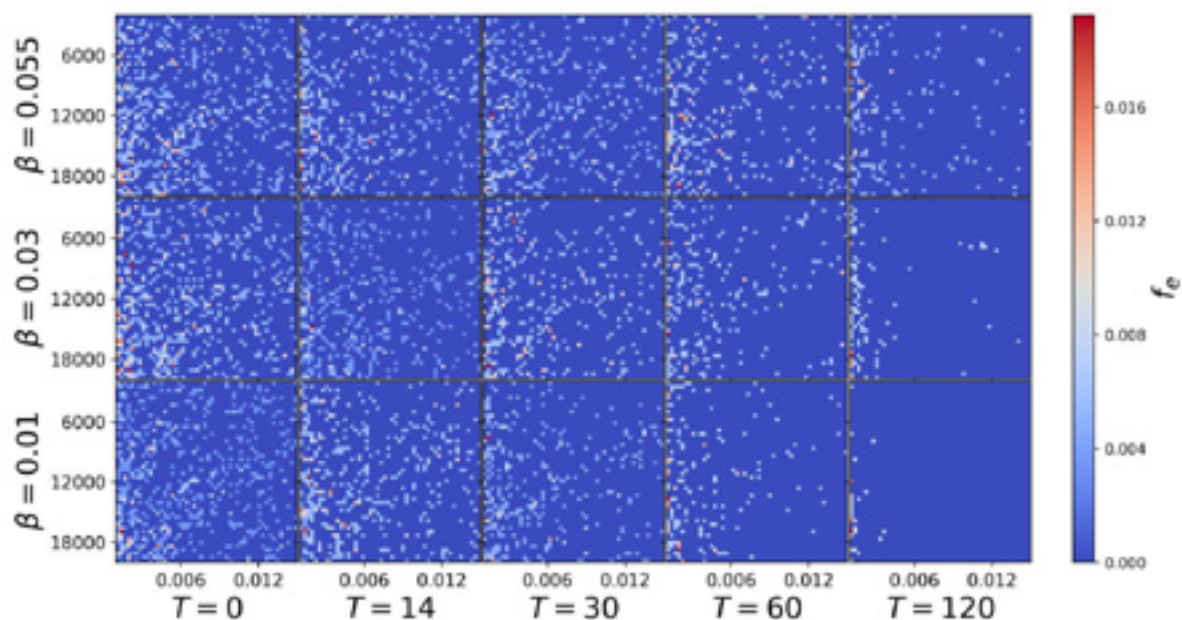


Figure S7 The probability of establishment of the resistant strain for $p = 10^{-8}$. The influence of low transmission period centered at $t/t_{v60} = 1$ on probability of establishment of the resistant strain as a function of the duration of that period, T , and the intensity of the reduction of transmission, β .

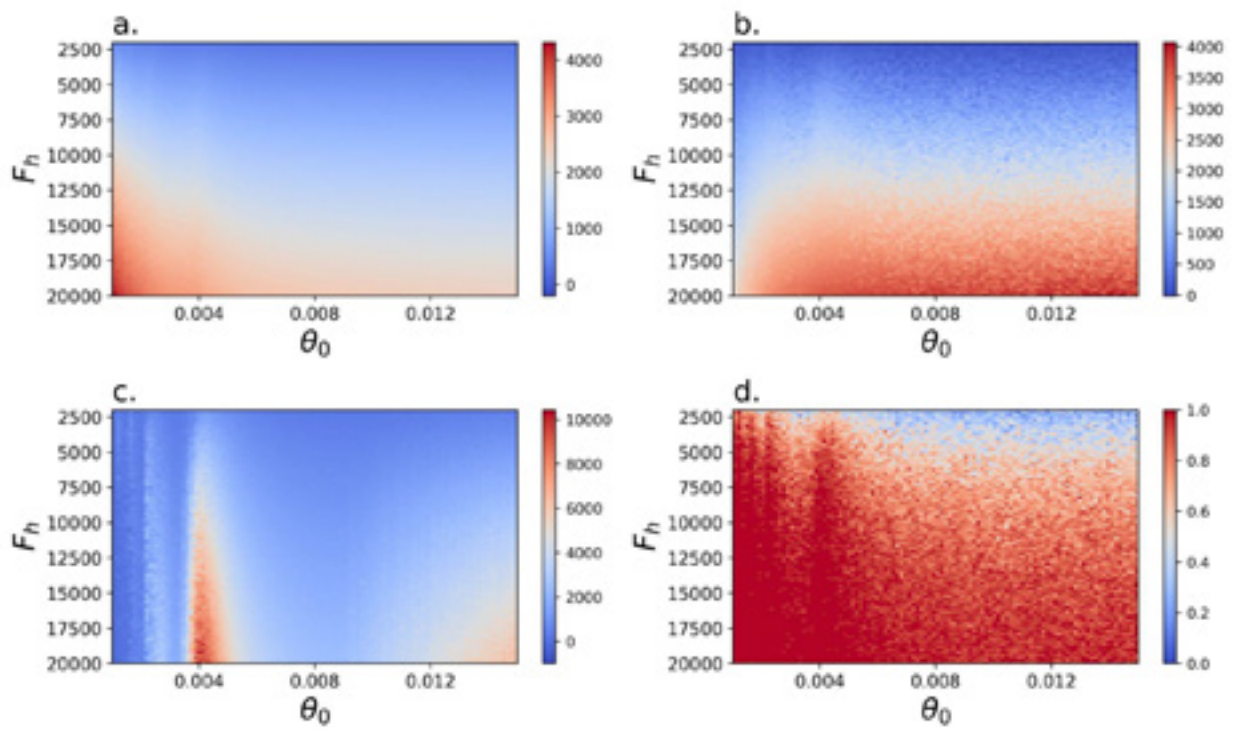


Figure S8 Impact of the rate of vaccination and initiation of low rate of transmission on model dynamics for $p = 10^{-5}$ and exit from low transmission at $F_i = F_h/8$. The cumulative death rate from the **a**, wildtype and **b**, resistant strains, **c**, the number of wildtype-strain infected individuals at t_{v60} , the point in time when 60% of the population is vaccinated and **d**, the probability of resistant strain establishment.

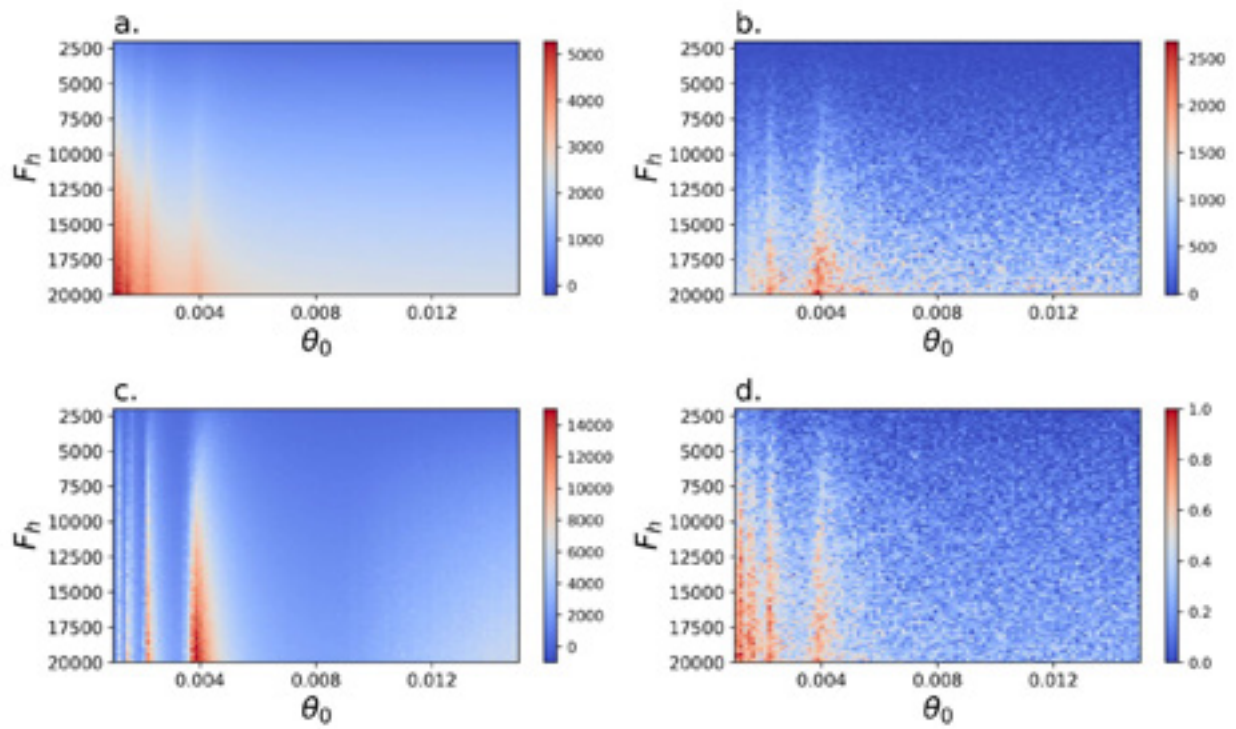


Figure S9 Impact of the rate of vaccination and initiation of low rate of transmission on model dynamics for $p = 10^{-6}$ and exit from low transmission at $F_i = F_h/8$. The cumulative death rate from the **a, wildtype and **b**, resistant strains, **c**, the number of wildtype-strain infected individuals at t_{v60} , the point in time when 60% of the population is vaccinated and **d**, the probability of resistant strain establishment.**

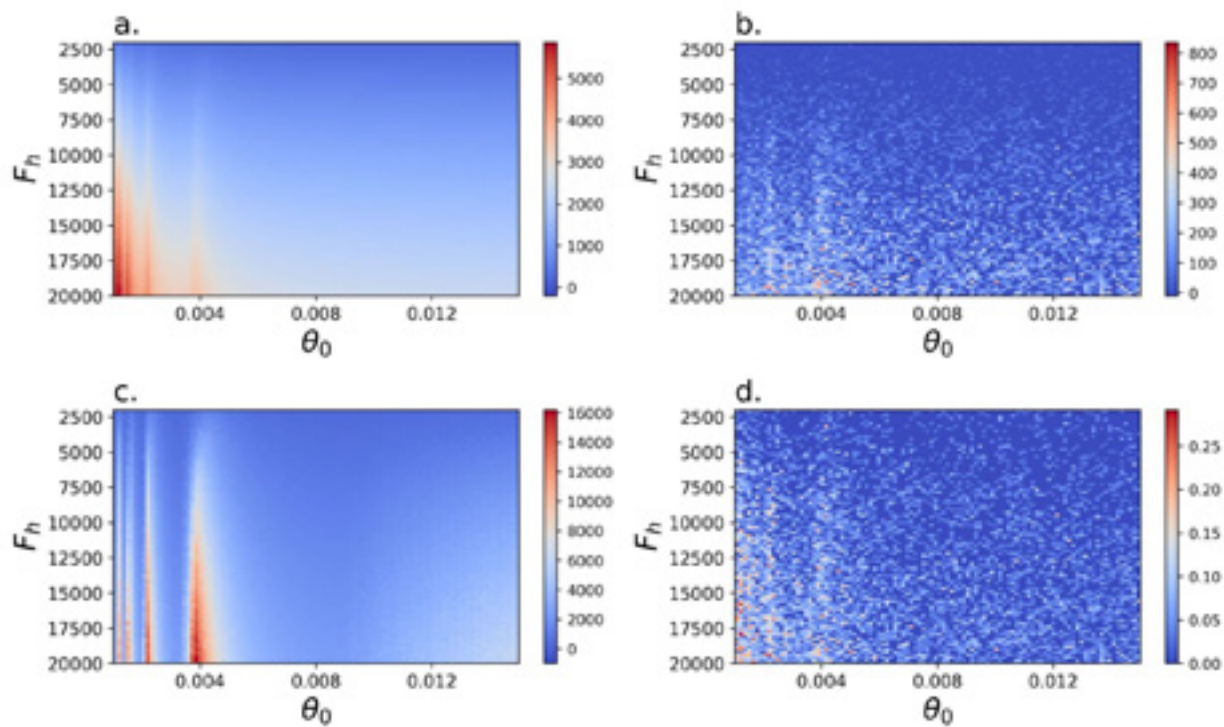


Figure S10 Impact of the rate of vaccination and initiation of low rate of transmission on model dynamics for $p = 10^{-7}$ and exit from low transmission at $F_l = F_h/8$. The cumulative death rate from the **a, wildtype and **b**, resistant strains, **c**, the number of wildtype-strain infected individuals at t_{v60} , the point in time when 60% of the population is vaccinated and **d**, the probability of resistant strain establishment.**

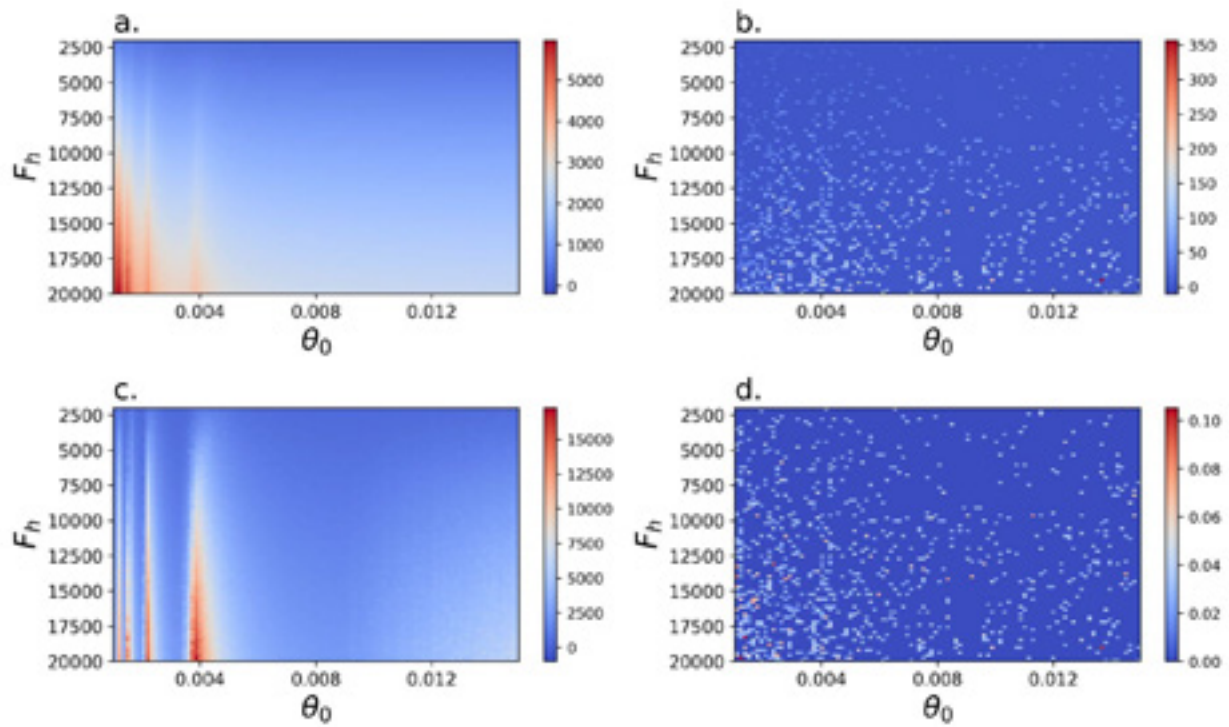


Figure S11 Impact of the rate of vaccination and initiation of low rate of transmission on model dynamics for $p = 10^{-8}$ and exit from low transmission at $F_r = F_h/8$. The cumulative death rate from the **a**, wildtype and **b**, resistant strains, **c**, the number of wildtype-strain infected individuals at t_{v60} , the point in time when 60% of the population is vaccinated and **d**, the probability of resistant strain establishment.

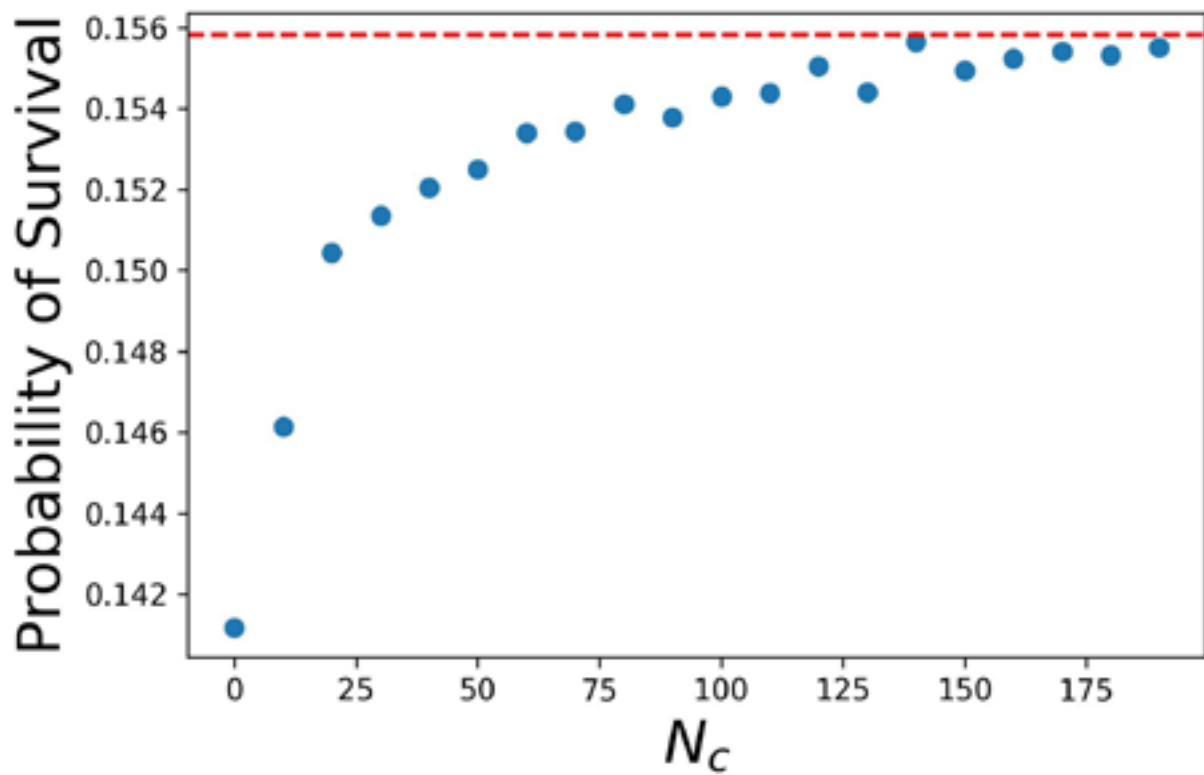


Figure S12. The fraction of surviving strains after $T=200$ days in 10^7 runs, first initialized with $I_{wt} = 200$ infected individuals. The red dashed line shows the expected fraction of surviving strains, as computed with eq. 13. The stochastic algorithm becomes exact, if no Tau Leaping is employed and instead the whole simulation is evaluated using the Gillespie SSA scheme.

BANCO DE ESPAÑA PUBLICATIONS

WORKING PAPERS

- 2010 ALFREDO GARCÍA-HIERNAUX, MARÍA T. GONZÁLEZ-PÉREZ and DAVID E. GUERRERO: Eurozone prices: a tale of convergence and divergence.
- 2011 ÁNGEL IVÁN MORENO BERNAL and CARLOS GONZÁLEZ PEDRAZ: Sentiment analysis of the Spanish Financial Stability Report. (There is a Spanish version of this edition with the same number).
- 2012 MARIAM CAMARERO, MARÍA DOLORES GADEA-RIVAS, ANA GÓMEZ-LOSCOS and CECILIO TAMARIT: External imbalances and recoveries.
- 2013 JESÚS FERNÁNDEZ-VILLAVERDE, SAMUEL HURTADO and GALO NUÑO: Financial frictions and the wealth distribution.
- 2014 RODRIGO BARBONE GONZALEZ, DMITRY KHAMETSHIN, JOSÉ-LUIS PEYDRÓ and ANDREA POLO: Hedger of last resort: evidence from Brazilian FX interventions, local credit, and global financial cycles.
- 2015 DANILO LEIVA-LEON, GABRIEL PEREZ-QUIROS and EYNO ROTS: Real-time weakness of the global economy: a first assessment of the coronavirus crisis.
- 2016 JAVIER ANDRÉS, ÓSCAR ARCE, JESÚS FERNÁNDEZ-VILLAVERDE and SAMUEL HURTADO: Deciphering the macroeconomic effects of internal devaluations in a monetary union.
- 2017 JACOPO TIMINI, NICOLA CORTINOVIS and FERNANDO LÓPEZ VICENTE: The heterogeneous effects of trade agreements with labor provisions.
- 2018 EDDIE GERBA and DANILO LEIVA-LEON: Macro-financial interactions in a changing world.
- 2019 JAIME MARTÍNEZ-MARTÍN and ELENA RUSTICELLI: Keeping track of global trade in real time.
- 2020 VICTORIA IVASHINA, LUC LAEVEN and ENRIQUE MORAL-BENITO: Loan types and the bank lending channel.
- 2021 SERGIO MAYORDOMO, NICOLA PAVANINI and EMANUELE TARANTINO: The impact of alternative forms of bank consolidation on credit supply and financial stability.
- 2022 ALEX ARMAND, PEDRO CARNEIRO, FEDERICO TAGLIATI and YIMING XIA: Can subsidized employment tackle long-term unemployment? Experimental evidence from North Macedonia.
- 2023 JACOPO TIMINI and FRANCESCA VIANI: A highway across the Atlantic? Trade and welfare effects of the EU-Mercosur agreement.
- 2024 CORINNA GHIRELLI, JAVIER J. PÉREZ and ALBERTO URTASUN: Economic policy uncertainty in Latin America: measurement using Spanish newspapers and economic spillovers.
- 2025 MAR DELGADO-TÉLLEZ, ESTHER GORDO, IVÁN KATARYNIUK and JAVIER J. PÉREZ: The decline in public investment: "social dominance" or too-rigid fiscal rules?
- 2026 ELVIRA PRADES-ILLANES and PATROCINIO TELLO-CASAS: Spanish regions in Global Value Chains: How important? How different?
- 2027 PABLO AGUILAR, CORINNA GHIRELLI, MATÍAS PACCE and ALBERTO URTASUN: Can news help measure economic sentiment? An application in COVID-19 times.
- 2028 EDUARDO GUTIÉRREZ, ENRIQUE MORAL-BENITO, DANIEL OTO-PERALÍAS and ROBERTO RAMOS: The spatial distribution of population in Spain: an anomaly in European perspective.
- 2029 PABLO BURRIEL, CRISTINA CHECHERITA-WESTPHAL, PASCAL JACQUINOT, MATTHIAS SCHÖN and NIKOLAI STÄHLER: Economic consequences of high public debt: evidence from three large scale DSGE models.
- 2030 BEATRIZ GONZÁLEZ: Macroeconomics, Firm Dynamics and IPOs.
- 2031 BRINDUSA ANGHEL, NÚRIA RODRÍGUEZ-PLANAS and ANNA SANZ-DE-GALDEANO: Gender Equality and the Math Gender Gap.
- 2032 ANDRÉS ALONSO and JOSÉ MANUEL CARBÓ: Machine learning in credit risk: measuring the dilemma between prediction and supervisory cost.
- 2033 PILAR GARCÍA-PEREA, AITOR LACUESTA and PAU ROLDAN-BLANCO: Raising Markups to Survive: Small Spanish Firms during the Great Recession.
- 2034 MÁXIMO CAMACHO, MATÍAS PACCE and GABRIEL PÉREZ-QUIRÓS: Spillover Effects in International Business Cycles.
- 2035 ÁNGEL IVÁN MORENO and TERESA CAMINERO: Application of text mining to the analysis of climate-related disclosures.
- 2036 EFFROSINI ADAMOPOULOU and ERNESTO VILLANUEVA: Wage determination and the bite of collective contracts in Italy and Spain: evidence from the metal working industry.
- 2037 MIKEL BEDAYO, GABRIEL JIMÉNEZ, JOSÉ-LUIS PEYDRÓ and RAQUEL VEGAS: Screening and Loan Origination Time: Lending Standards, Loan Defaults and Bank Failures.
- 2038 BRINDUSA ANGHEL, PILAR CUADRADO and FEDERICO TAGLIATI: Why cognitive test scores of Spanish adults are so low? The role of schooling and socioeconomic background

- 2039 CHRISTOPH ALBERT, ANDREA CAGGESE and BEATRIZ GONZÁLEZ: The Short- and Long-run Employment Impact of COVID-19 through the Effects of Real and Financial Shocks on New Firms.
- 2040 GABRIEL JIMÉNEZ, DAVID MARTÍNEZ-MIERA and JOSÉ-LUIS PEYDRÓ: Who Truly Bears (Bank) Taxes? Evidence from Only Shifting Statutory Incidence.
- 2041 FELIX HOLUB, LAURA HOSPIDO and ULRICH J. WAGNER: Urban air pollution and sick leaves: evidence from social security data.
- 2042 NÉLIDA DÍAZ SOBRINO, CORINNA GHIRELLI, SAMUEL HURTADO, JAVIER J. PÉREZ and ALBERTO URTASUN: The narrative about the economy as a shadow forecast: an analysis using Banco de España quarterly reports.
- 2043 NEZIH GUNER, JAVIER LÓPEZ-SEGOVIA and ROBERTO RAMOS: Reforming the individual income tax in Spain.
- 2101 DARÍO SERRANO-PUENTE: Optimal progressivity of personal income tax: a general equilibrium evaluation for Spain.
- 2102 SANDRA GARCÍA-URIBE, HANNES MUELLER and CARLOS SANZ: Economic uncertainty and divisive politics: evidence from the *Dos Españas*.
- 2103 IVÁN KATARYNIUK, VÍCTOR MORA-BAJÉN and JAVIER J. PÉREZ: EMU deepening and sovereign debt spreads: using political space to achieve policy space.
- 2104 DARÍO SERRANO-PUENTE: Are we moving towards an energy-efficient low-carbon economy? An input-output LMDI decomposition of CO₂ emissions for Spain and the EU28.
- 2105 ANDRÉS ALONSO and JOSÉ MANUEL CARBÓ: Understanding the performance of machine learning models to predict credit default: a novel approach for supervisory evaluation.
- 2106 JAVIER ANDRÉS, ÓSCAR ARCE and PABLO BURRIEL: Market polarization and the Phillips curve.
- 2107 JUAN de LUCIO and JUAN S. MORA-SANGUINETTI: New dimensions of regulatory complexity and their economic cost. An analysis using text mining.
- 2108 DANILO LEIVA-LEON and LUIS UZEDA: Endogenous time variation in vector autoregressions.
- 2109 CORINNA GHIRELLI, ANDREA GONZÁLEZ, JOSÉ LUIS HERRERA and SAMUEL HURTADO: Weather, mobility and the evolution of the Covid-19 pandemic.
- 2110 KLODIANA ISTREFI, FLORENS ODENDAHL and GIULIA SESTIERI: Fed communication on financial stability concerns and monetary policy decisions: revelations from speeches.
- 2111 YUNUS AKSOY, HENRIQUE S. BASSO and CAROLYN ST AUBYN: Time Variation in Lifecycle Consumption and Income.
- 2112 JENNIFER PEÑA and ELVIRA PRADES: Price setting in Chile: micro evidence from consumer on-line prices during the social outbreak and Covid-19.
- 2113 NEZIH GUNER, YULIYA A. KULIKOVA and ARNAU VALLADARES-ESTEBAN: Does the added worker effect matter?
- 2114 RODOLFO G. CAMPOS and JACOPO TIMINI: Unequal trade, unequal gains: the heterogeneous impact of MERCOSUR.
- 2115 JAVIER QUINTANA: Import competition, regional divergence, and the rise of the skilled city.
- 2116 PATRICK MACNAMARA, MYROSLAV PIDKUYKO and RAFFAELE ROSSI: Marginal Tax Changes with Risky Investment.
- 2117 RODOLFO G. CAMPOS, JACOPO TIMINI and ELENA VIDAL: Structural gravity and trade agreements: does the measurement of domestic trade matter?
- 2118 ALESSANDRO MELCARNE, JUAN S. MORA-SANGUINETTI and ROK SPRUK: Democracy, technocracy and economic growth: evidence from 20 century Spain.
- 2119 ÁNGEL ESTRADA and DANIEL SANTABÁRBARA: Recycling carbon tax revenues in Spain. Environmental and economic assessment of selected green reforms.
- 2120 ALEJANDRO FERNÁNDEZ-CEREZO, BEATRIZ GONZÁLEZ, MARIO IZQUIERDO and ENRIQUE MORAL-BENITO: Firm-level heterogeneity in the impact of the COVID-19 pandemic.
- 2121 EDUARDO GUTIÉRREZ and CÉSAR MARTÍN MACHUCA: The effect of tariffs on Spanish goods exports.
- 2122 JACOPO TIMINI: Revisiting the 'Cobden-Chevalier network' trade and welfare effects.
- 2123 ALEJANDRO BUESA, JAVIER J. PÉREZ and DANIEL SANTABÁRBARA: Awareness of pandemics and the impact of COVID-19.
- 2124 ALICIA AGUILAR and DIEGO TORRES: The impact of COVID-19 on analysts' sentiment about the banking sector.
- 2125 SILVIA ALBRIZIO, IVÁN KATARYNIUK, LUIS MOLINA and JAN SCHÄFER: ECB euro liquidity lines.
- 2126 ANTHONY BALD, ERIC CHYN, JUSTINE HASTINGS and MARGARITA MACHELETT: The causal impact of removing children from abusive and neglectful homes.
- 2127 IRMA ALONSO, PEDRO SERRANO and ANTONI VAELO-SEBASTIÀ: The impact of heterogeneous unconventional monetary policies on the expectations of market crashes.
- 2128 MARÍA T. GONZÁLEZ-PÉREZ: Lessons from estimating the average option-implied volatility term structure for the Spanish banking sector.
- 2129 SIMÓN A. RELLA, YULIYA A. KULIKOVA, EMMANOUIL T. DERMITZAKIS and FYODOR A. KONDRASHOV: Rates of SARS-COV-2 transmission and vaccination impact the fate of vaccine-resistant strains.